Perspective of vector charmonium-like states at STCF in coupled-channel analysis

arXiv: 2312.17658v3

Satoshi Nakamura (Shandong Univ.)

Collaborators: X.-H. Li, H.-P. Peng, X.-R. Zhou (USTC), Z.-T. Sun (SDU)

Introduction

From BESIII to STCF

BESIII as vector-charmonium factory

Advantage of direct production

compared to ISR method

High-precision study of exotic Y states

$e^+e^- \to J/\psi\,\pi^+\pi^-$ →

PRL 118, 092001 (2017)

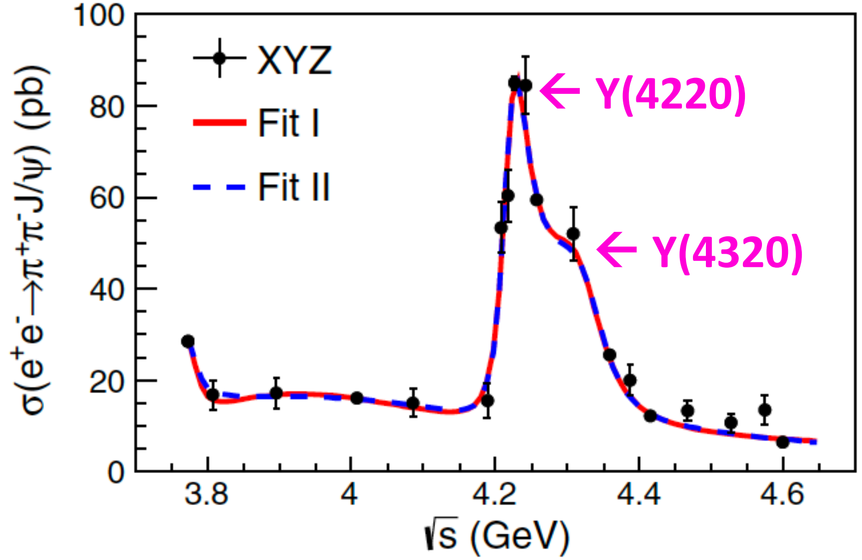

$e^+e^- \to \pi^+ D^0 D^{*-}$ PRL 122, 102002 (2019)

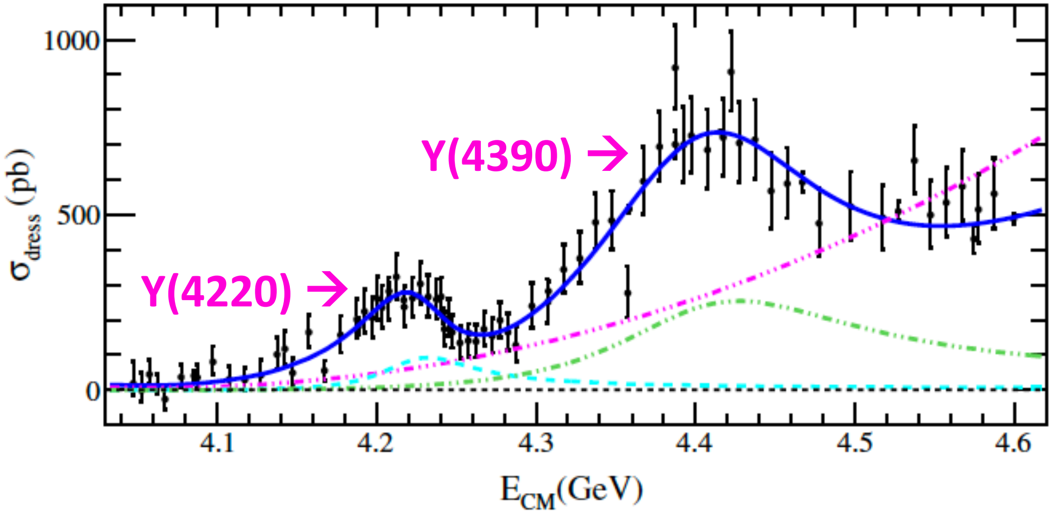

PRD 102, 031101 (2020)

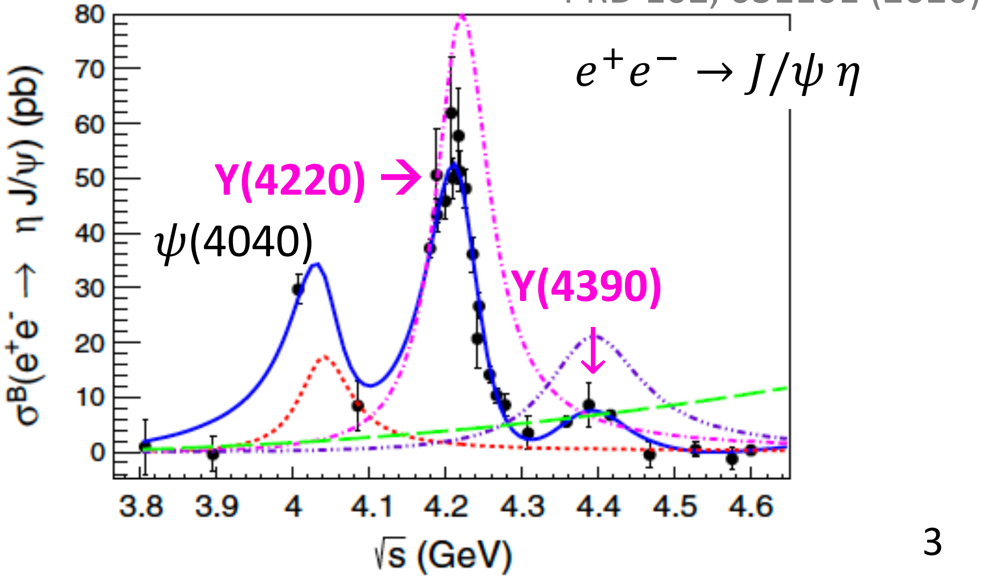

BESIII accumulated high-precision cross-section data for various final states

→ Coupled-channel analysis for determining vector charmonium poles

Our combined analysis of BESIII and Belle data for various $e^+e^- \to c\bar{c}$ processes over $3.75 \leq \sqrt{s} \leq 4.7$ GeV

$e^+e^- \to D^{(*)}\overline{D}^{(*)}, D_s^{(*)}\overline{D}_s^{(*)}, J/\psi\, \eta^{(\prime)}, \chi_{c0}\omega, \Lambda_c\overline{\Lambda}_c$ (10 two-body final states)

$e^+e^- \to \pi D^{(*)}\overline{D}^{(*)},\ J/\psi\pi\pi,\ \psi'\pi\pi, h_c\pi\pi, J/\psi K\overline{K}$ (7 three-body final states)

$e^+e^- \to \eta_c\rho\pi\ (\rho \to \pi\pi)$ (1 four-body final states)

- Approximate three-body unitarity model
- Fit both cross sections and invariant mass distributions
- Extract vector charmonium and Zc poles
- Compositeness → identify hadron-molecule-dominated states

STCF will significantly advance coupled-channel analysis

	BESIII	→	STCF
$\sqrt{s}$ (charmonium region)	3—5 GeV		3—7 GeV
$\mathcal{L}$ (Luminosity)			$\sim 50 \times \mathcal{L}$ (BESIII)

- Wider $\sqrt{s}$ coverage → discovery potential of heavier (vector) charmonium states
- Higher $\mathcal{L}$ -- more precise data
  → more precise determinations of charmonium poles and residues (statistical improvement)

  -- more detailed data (Dalitz plots and angle distribution at each $\sqrt{s}$, etc.)

  → less model-dependent charmonium poles and residues (systematics improvement)

  → more detailed charmonium properties: branching ratios, compositeness

This talk

- (short) review of our coupled-channel analysis of BESIII $e^+e^- \to c\bar{c}$ data

  -- Theoretical framework

  -- Result on fit

  -- Result on vector charmonium poles, compositeness

- Along with the analysis result, expected improvements with STCF data will be discussed

MODEL

Full amplitude for e^+e^- → three-body final states

Dressed vertices (propagator) : bare vertices (propagator) dressed by hadron scattering

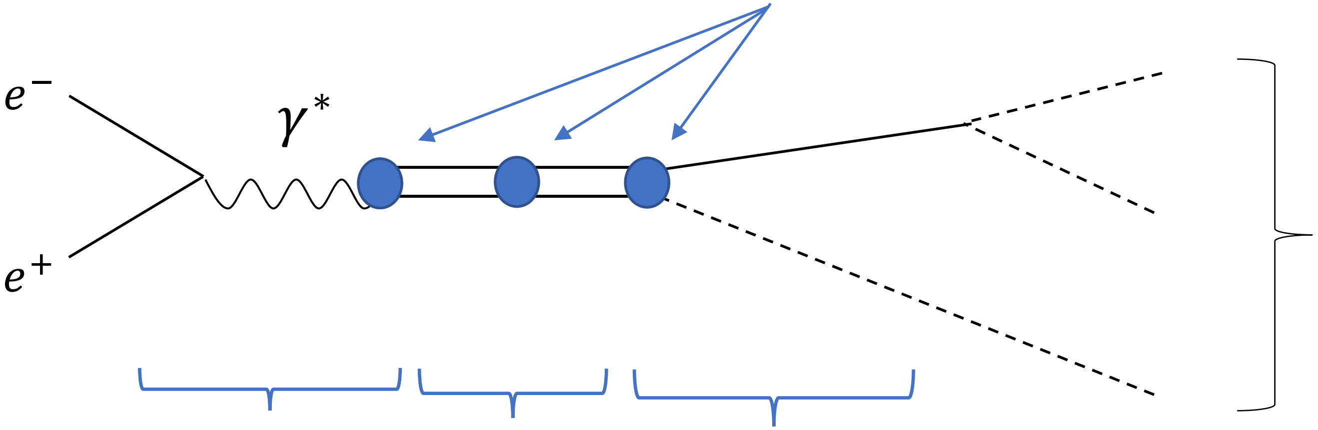

Unitarity requirement

$\pi D^{(*)}\bar{D}^{(*)},\ J/\psi\pi\pi,\ \psi'\pi\pi, h_c\pi\pi, \eta_c\rho\pi, J/\psi K\bar{K}$

ψ production,   propagation,   decay

Non-resonant mechanisms are also included (no ψ excitations)

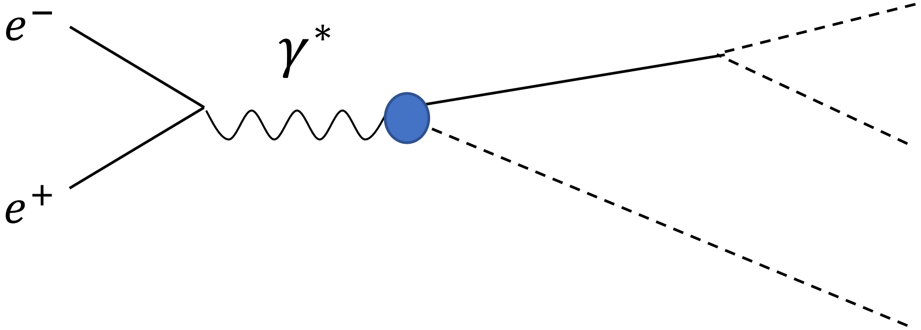

Coupled-channels

(quasi) two-body channels included; $J^{PC} = 1^{--}$

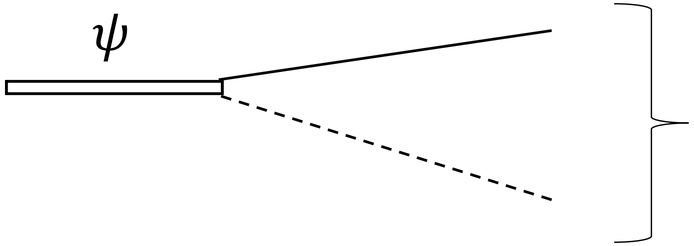

$D_1(2420)\bar{D}^{(*)}$, $D_1(2430)\bar{D}^{(*)}$, $D_2^*(2460)\bar{D}^{(*)}$, $D^{(*)}\bar{D}^{(*)}$, $D_{s1}(2536)\bar{D}_s$

$\omega\chi_{c0}$, $D_s^{(*)}\bar{D}_s^{(*)}$, $\Lambda_c\bar{\Lambda}_c$, $D_0^*(2300)\bar{D}^*$, $f_0\, J/\psi$, $Z_c\pi$, … etc.

These channels couple with each other through:

- Charmonium excitations

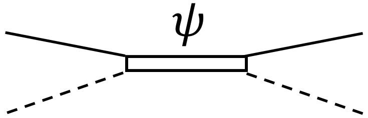

- (potentially on-shell) particle-exchange mechanisms

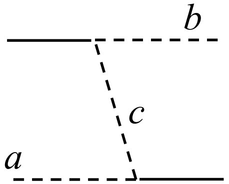

- Short-range mechanisms

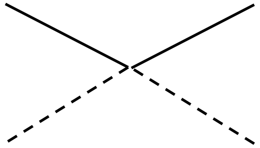

Three-body decays of ψ

$D_1\overline{D}$ and $D_1\overline{D}^*$ molecule states included

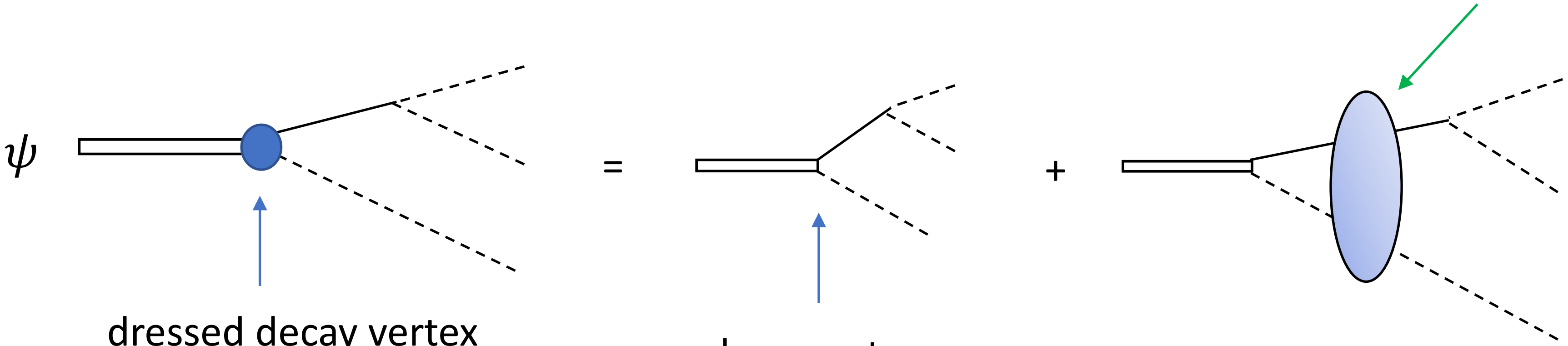

dressed decay vertex

bare vertex

rescattering terms (final-state interactions)

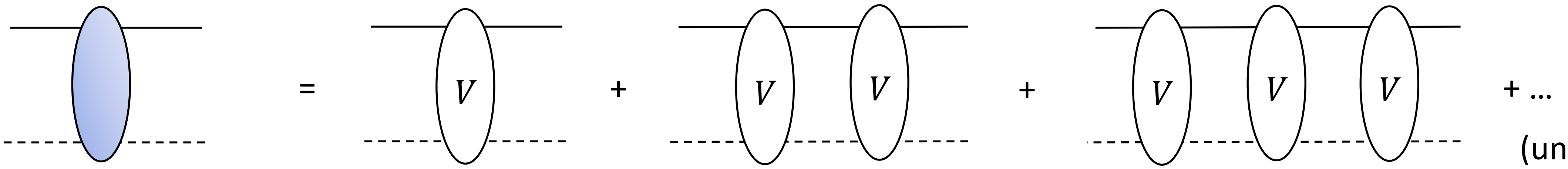

(until infinite loops)

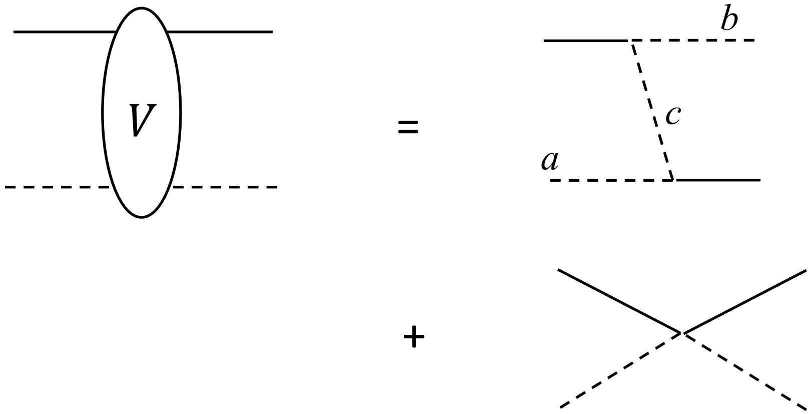

(on-shell) particle-exchange mechanisms → three-body unitarity

$$\propto \frac{1}{E - E_a - E_b - E_c}$$

Short-range mechanisms among open-charm channels (E-independent)

ψ propagator

(we do not use BW)

($D^*\pi$-loop is replaced by D_1 BW)

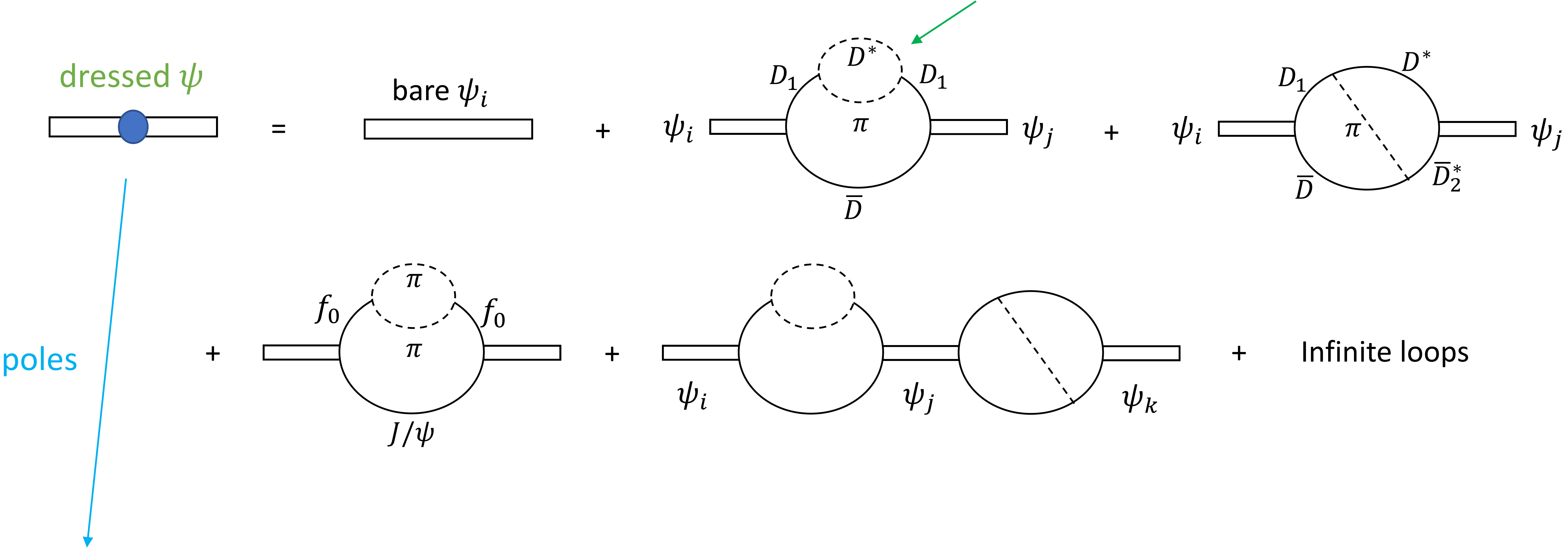

Charmonium poles from non-perturbative couplings between bare ψ and $D_1\bar{D}$, $f_0\,J/\psi$, ...

Unitary coupled-channel model : resonance pole (mass, width) and decay dynamics are explicitly related.

(unitarity requirement)

Breit-Wigner model : decay dynamics are simulated by BW mass and width parameters

Selected fit results

$e^+e^- \to J/\psi\,\pi^+\pi^-, J/\psi\,\pi^0\pi^0$

Data: BESIII,
PRD 106, 072001 (2022)
PRD 102, 012009 (2020)

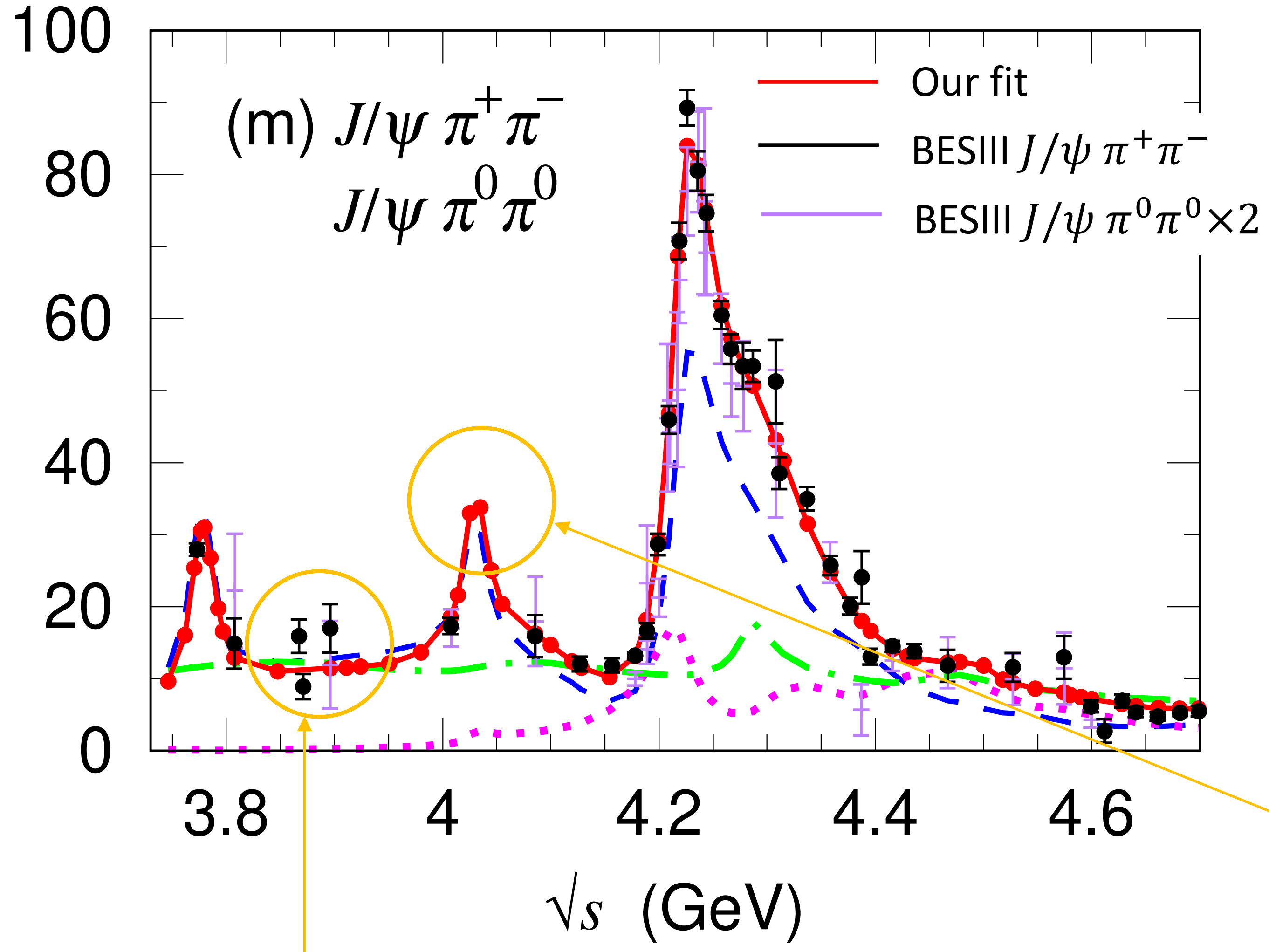

- Peaking structure at $\sqrt{s} \sim 4$ GeV is from $\psi(4040)$

→ consequence of the combined fit

Can be confirmed by STCF

Dip due to X(3872) ? Baru et al. PRD (2024)

→ The dip can be confirmed by STCF

$e^+e^- \to J/\psi\,\pi^+\pi^-$

Data: BESIII, PRL 119, 072001 (2017)

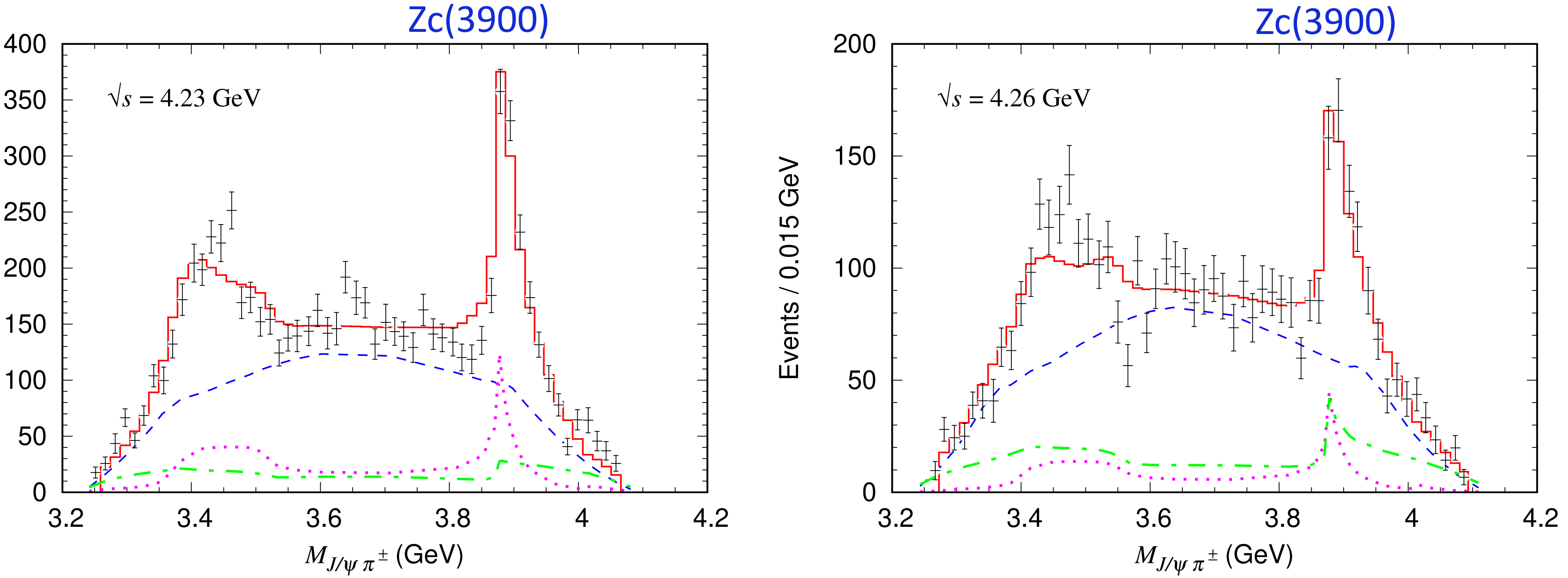

direct decay

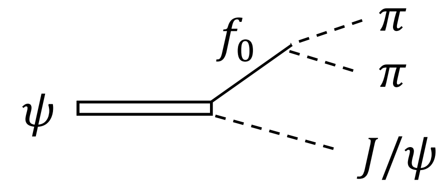

1-triangle

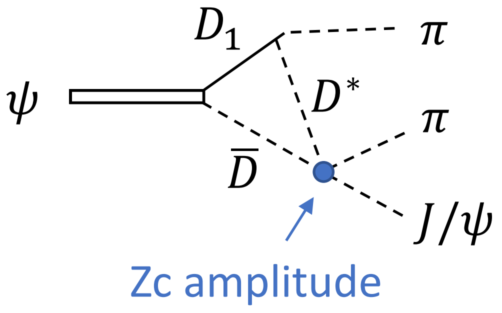

1-loop causes $D^*\bar{D}$ thres. cusp enhanced by Zc pole

triangle singularity (TS) occurs at $\sqrt{s} \sim 4.28$ GeV ($\Gamma_{D_1} = 30$ MeV)

STCF : extensive study on $\sqrt{s}$-dependence of the lineshape

→ Disentangle TS and $D^*\bar{D}$ cusp effects

→ More constraints on Zc pole location, $\psi(4230) \to D_1\bar{D}$ coupling, $D_1\bar{D}$ molecule contents in $\psi(4230)$

$e^+e^- \to \Lambda_c\overline{\Lambda}_c$, $\pi D^*\overline{D}^*$

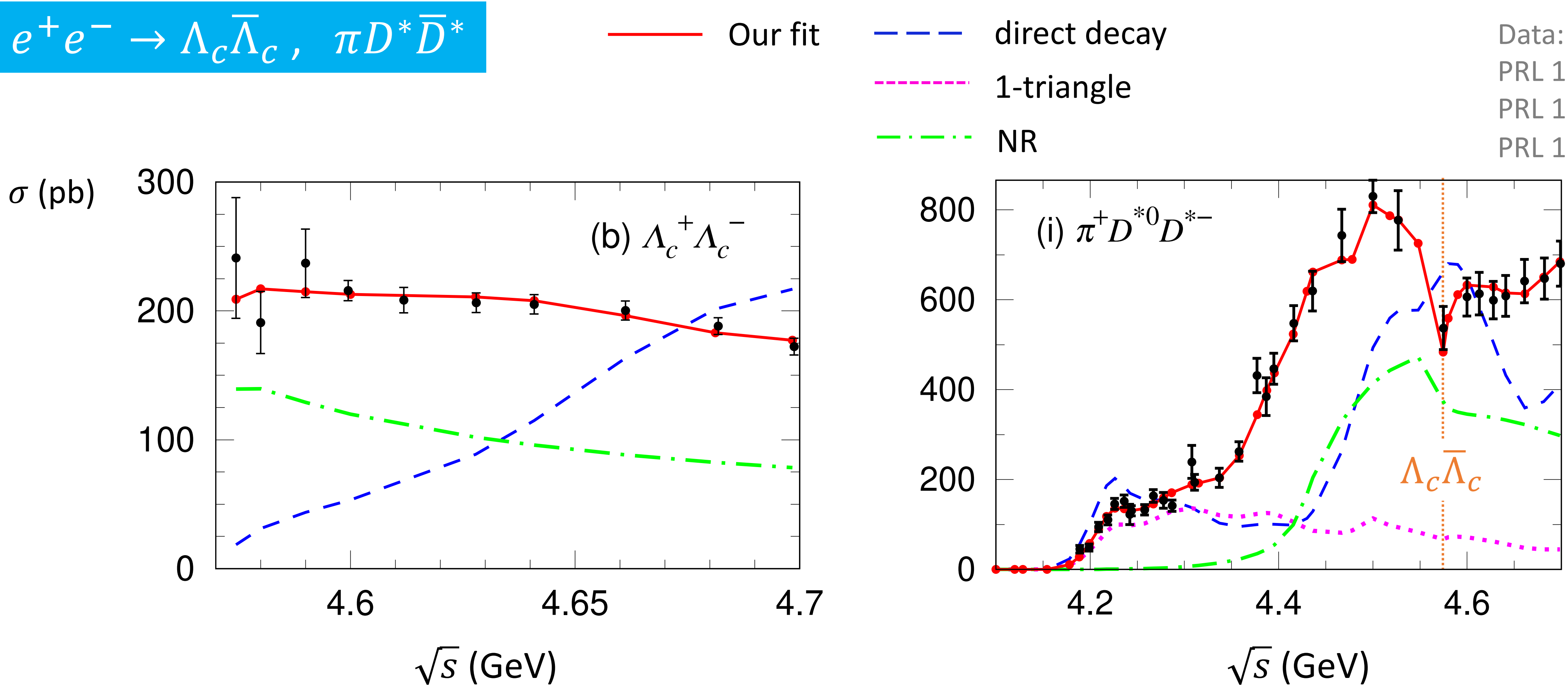

Data: BESIII,
PRL 120, 132001 (2018)
PRL 131, 191901 (2023)
PRL 130, 121901 (2023)

- $\Lambda_c\overline{\Lambda}_c$ threshold enhancement ← attractive $\Lambda_c\overline{\Lambda}_c$ interaction (pole near threshold is likely)
- $\Lambda_c\overline{\Lambda}_c$ threshold cusp is important to fit $e^+e^- \to \pi D^*\overline{D}^*$ data at $\sqrt{s} \sim 4.57$ GeV ← STCF confirms the dip
- **STCF** will measure more baryonic channels, $\Sigma_c\bar{\Sigma}_c$, $\Lambda_c(2595)\overline{\Lambda}_c$, etc. and threshold enhancements (nearby poles)

Importance of threshold effects to understand charmonium mass

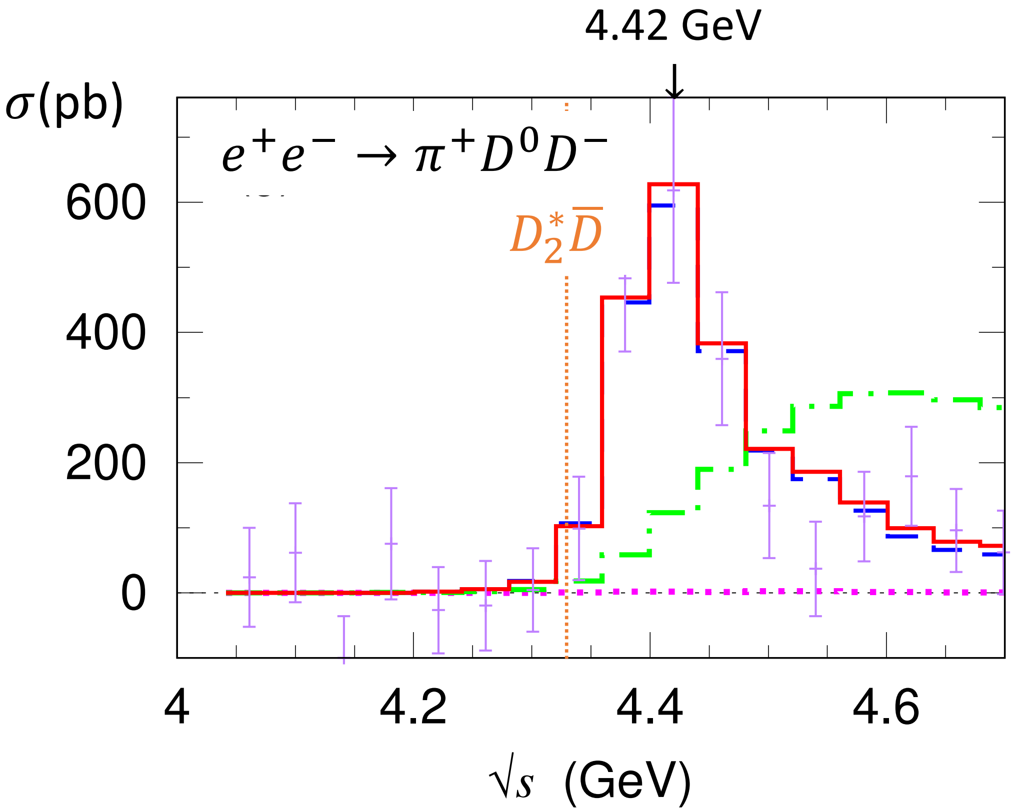

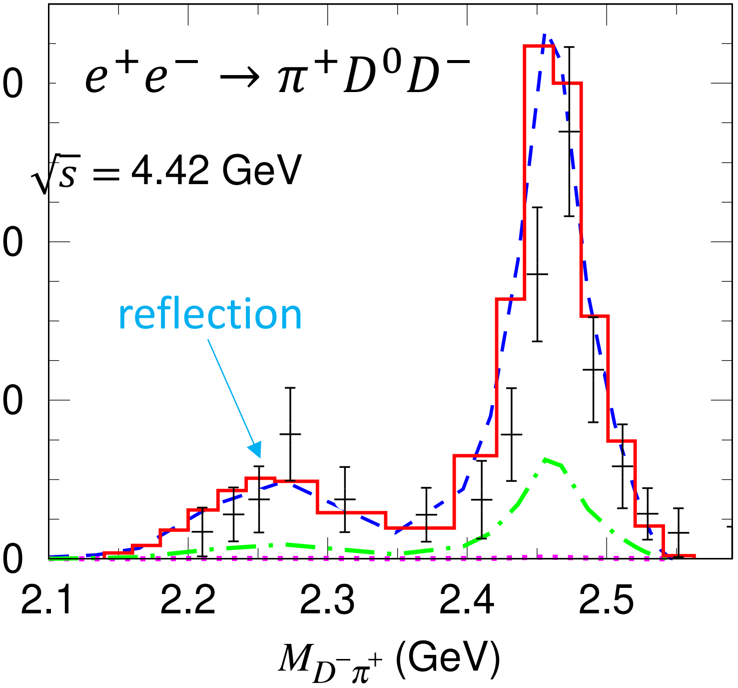

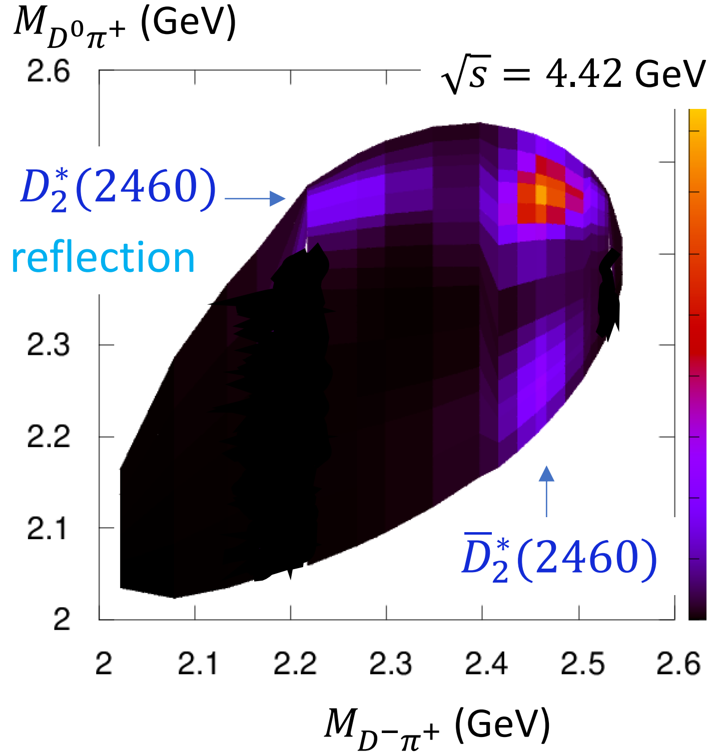

Decay sequence:

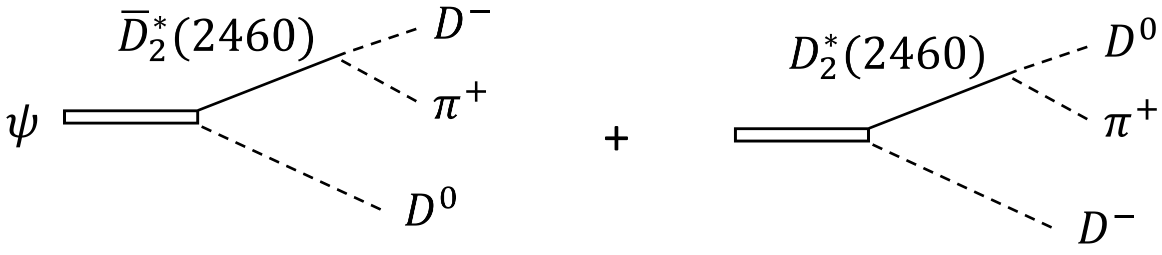

Importance of threshold effects to understand charmonium mass

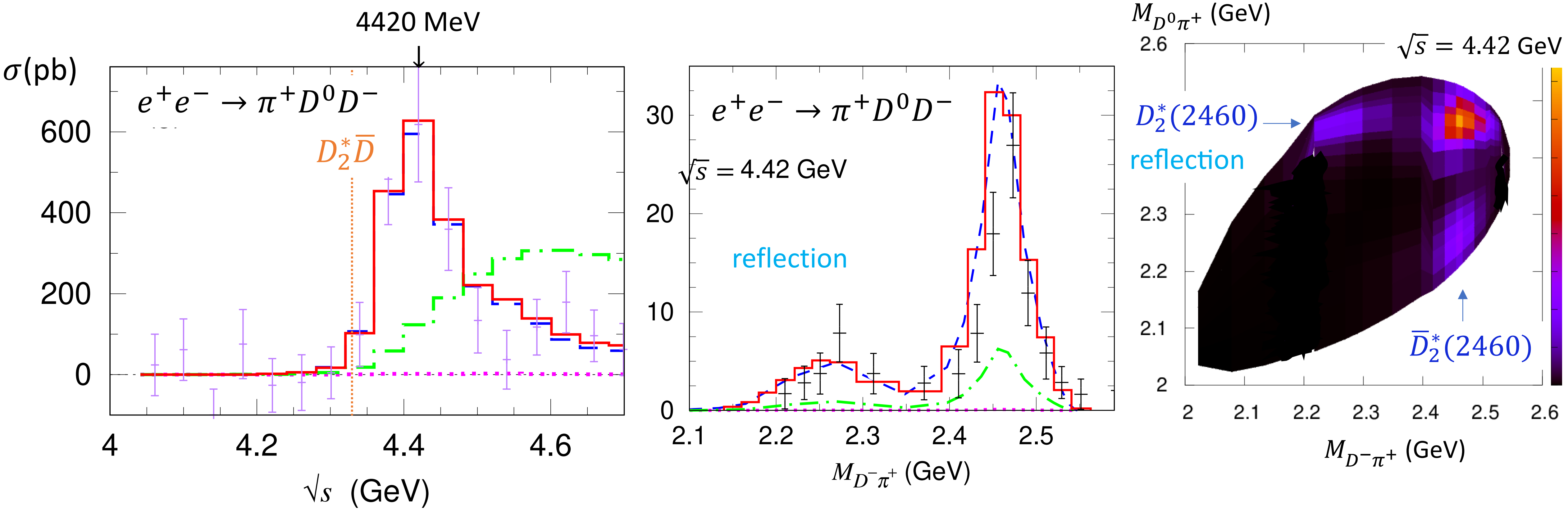

- This process is strongly suppressed below $D_2^*\bar{D}$ threshold (Γ_{D_2}~47 MeV)
- $D_2^*\bar{D}$ channel is d-wave → centrifugal barrier suppression near threshold
- Peak position is shifted from pole position ($M_{\rm pole}$=4390 MeV) by ~30 MeV to higher $\sqrt{s}$
- Fit cross-section (σ) data with $|A_{BW}|^2\times$ ($\pi D\bar{D}$ phase-space) is not justified ($M_{\rm BW}$=4420 MeV ← artifact)

Importance of threshold effects to understand charmonium mass

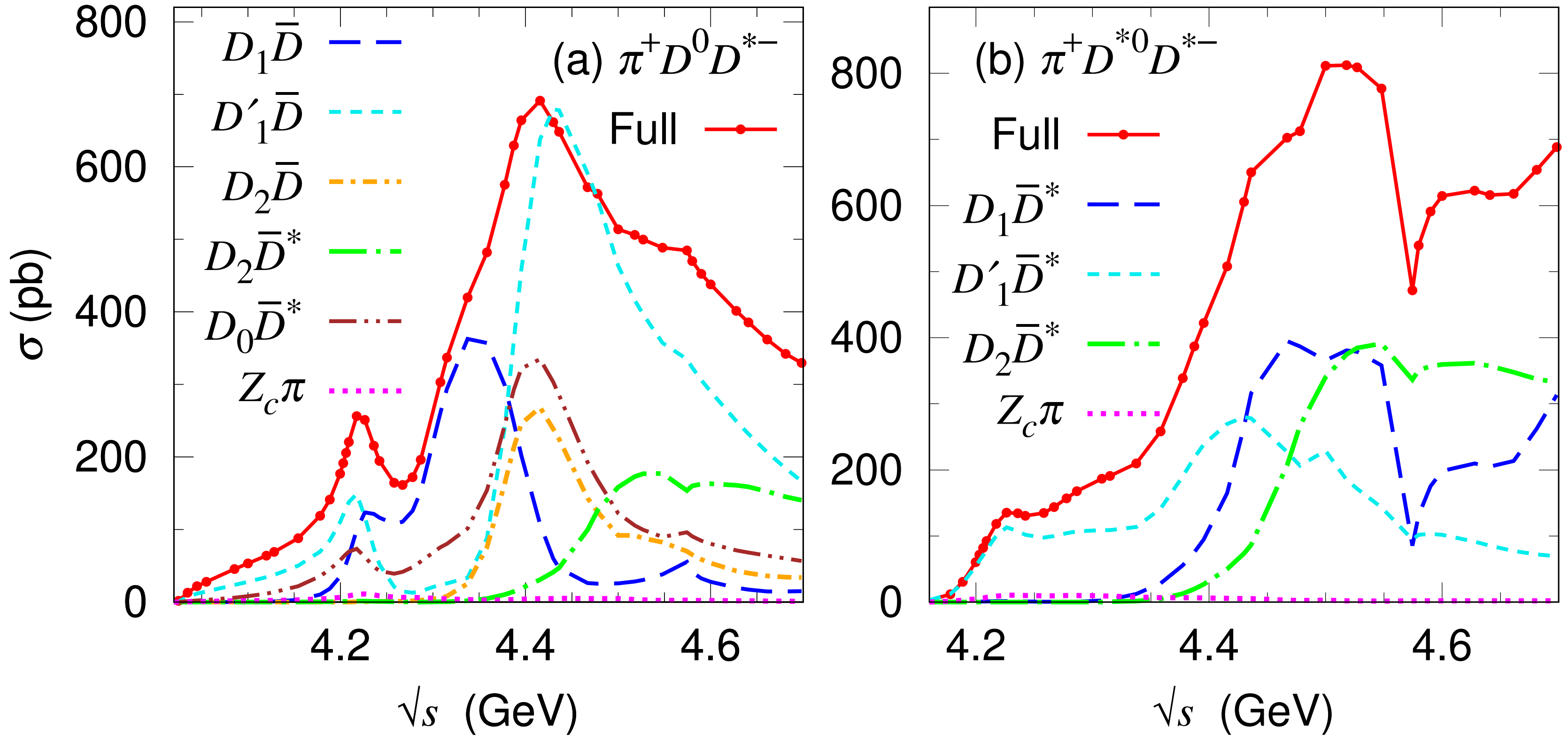

Sub-process

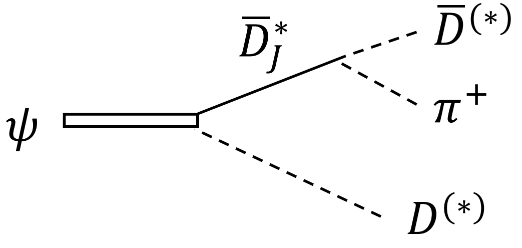

- Each sub-process is suppressed below $D_J^*\bar{D}^{(*)}$ threshold (if Γ_{D_J} is narrow)

- Peak positions (lineshape) can be shifted from pole locations by threshold effects
- Fit cross-section data (σ) with $|A_{BW}|^2\times$ (phase-space) is not justified
- Dalitz-plot data is important to constrain $D_J^*\bar{D}^{(*)}$ contributions and correctly find pole locations → **STCF can provide detailed data**

Poles and resonance properties

Pole locations

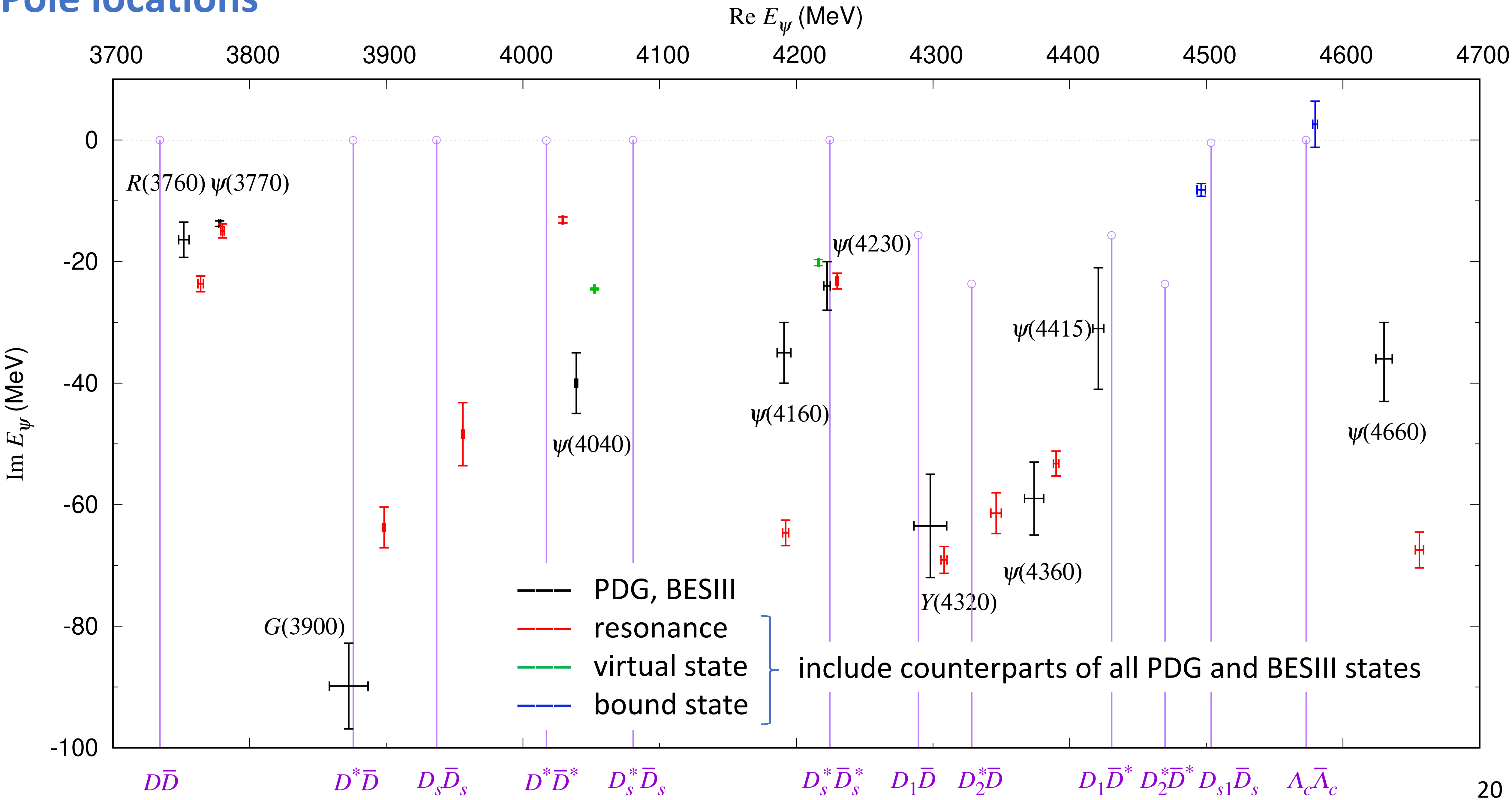

include counterparts of all PDG and BESIII states

Pole locations

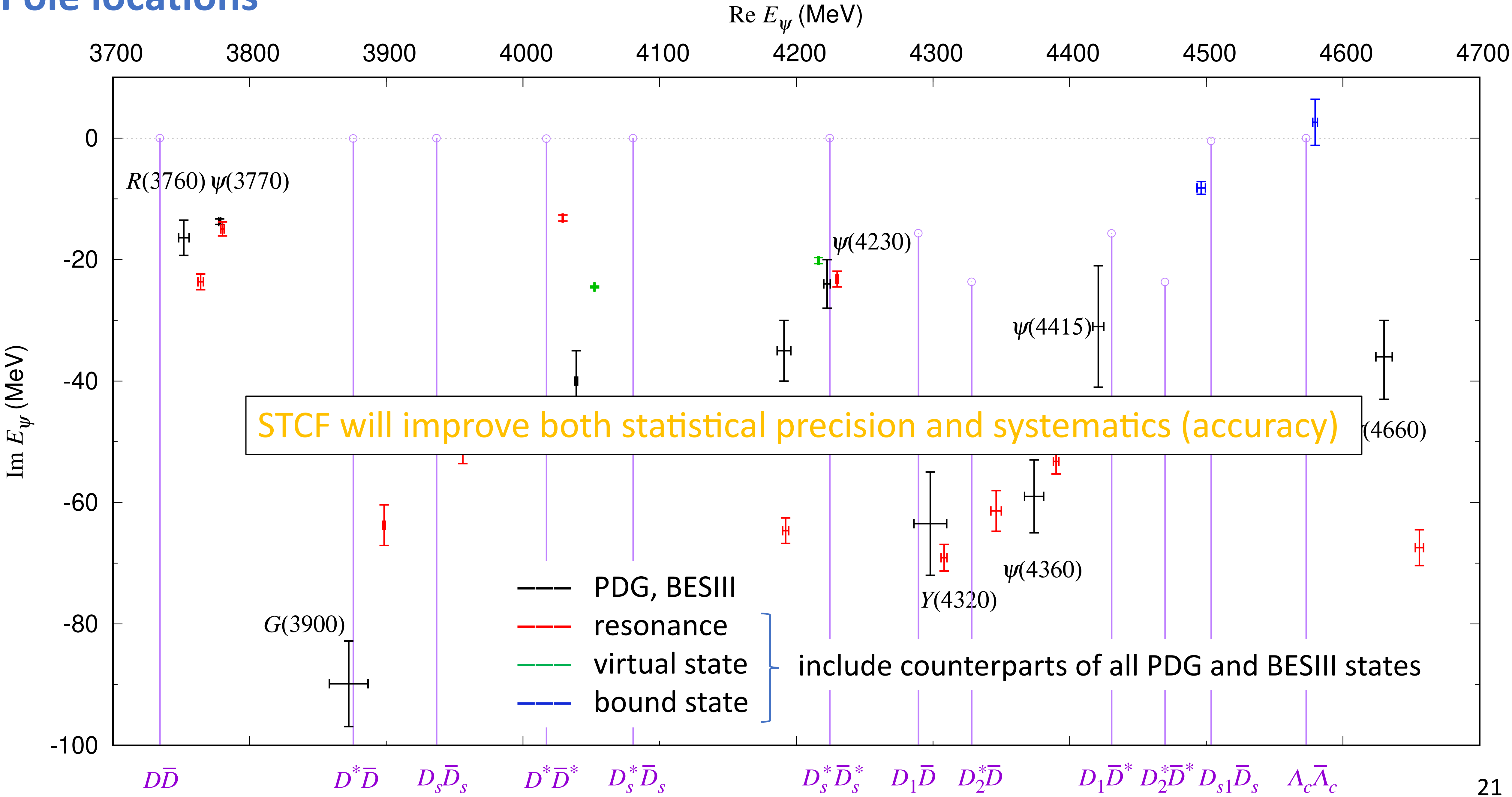

STCF will improve both statistical precision and systematics (accuracy)

include counterparts of all PDG and BESIII states

Compositeness

Hadron-molecule content in vector charmonium states

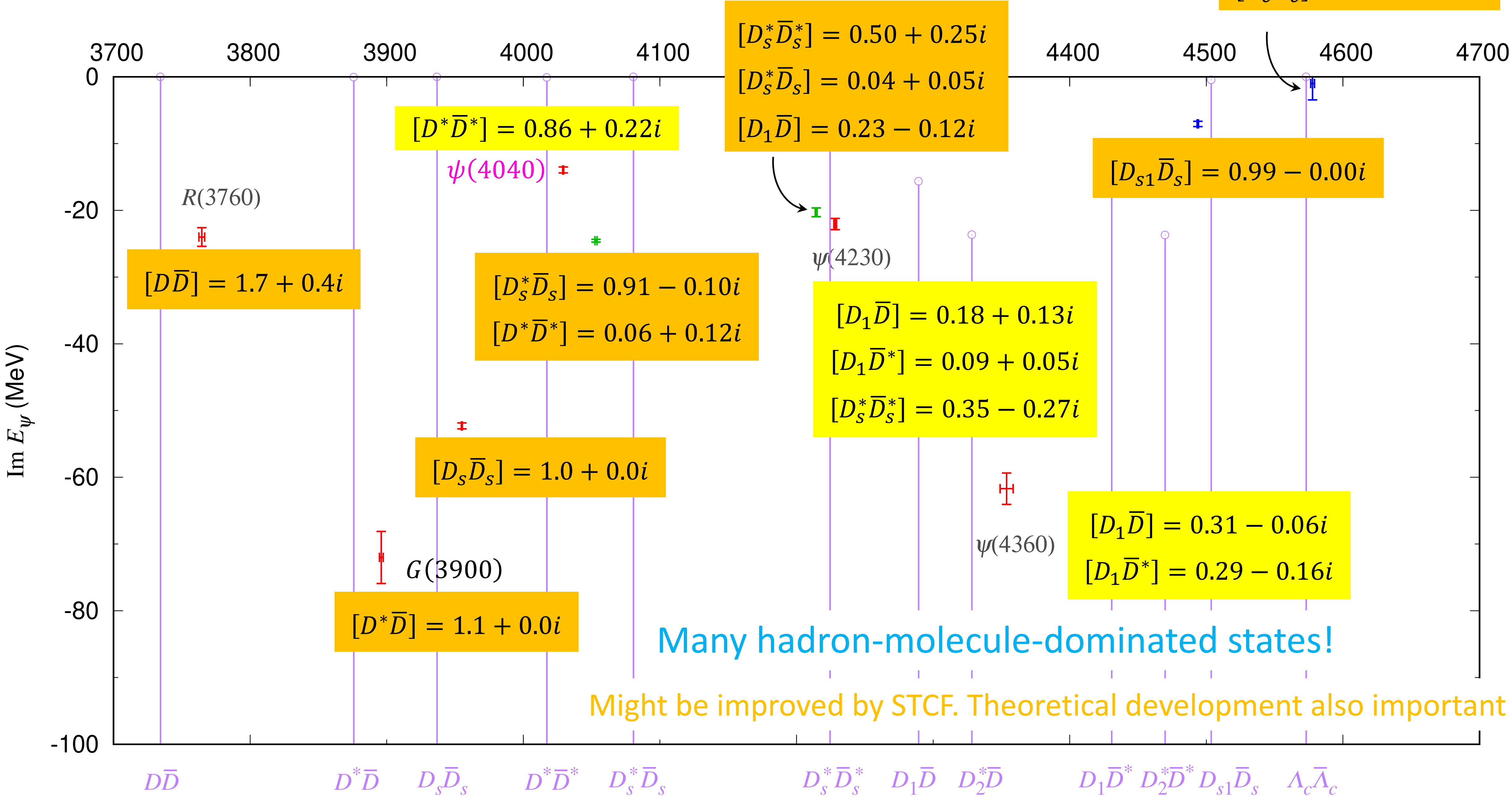

$[\Lambda_c\bar{\Lambda}_c] = 0.97 + 0.01i$

$[D_s^*\bar{D}_s^*] = 0.50 + 0.25i$

$[D_s^*\bar{D}_s] = 0.04 + 0.05i$

$[D_1\bar{D}] = 0.23 - 0.12i$

$[D^*\bar{D}^*] = 0.86 + 0.22i$

$[D_{s1}\bar{D}_s] = 0.99 - 0.00i$

$[D\bar{D}] = 1.7 + 0.4i$

$[D_s^*\bar{D}_s] = 0.91 - 0.10i$

$[D^*\bar{D}^*] = 0.06 + 0.12i$

$[D_1\bar{D}] = 0.18 + 0.13i$

$[D_1\bar{D}^*] = 0.09 + 0.05i$

$[D_s^*\bar{D}_s^*] = 0.35 - 0.27i$

$[D_s\bar{D}_s] = 1.0 + 0.0i$

$[D_1\bar{D}] = 0.31 - 0.06i$

$[D_1\bar{D}^*] = 0.29 - 0.16i$

$[D^*\bar{D}] = 1.1 + 0.0i$

Many hadron-molecule-dominated states!

Might be improved by STCF. Theoretical development also important

Charmonium spectrum ($J^{PC} = 1^{--}$)

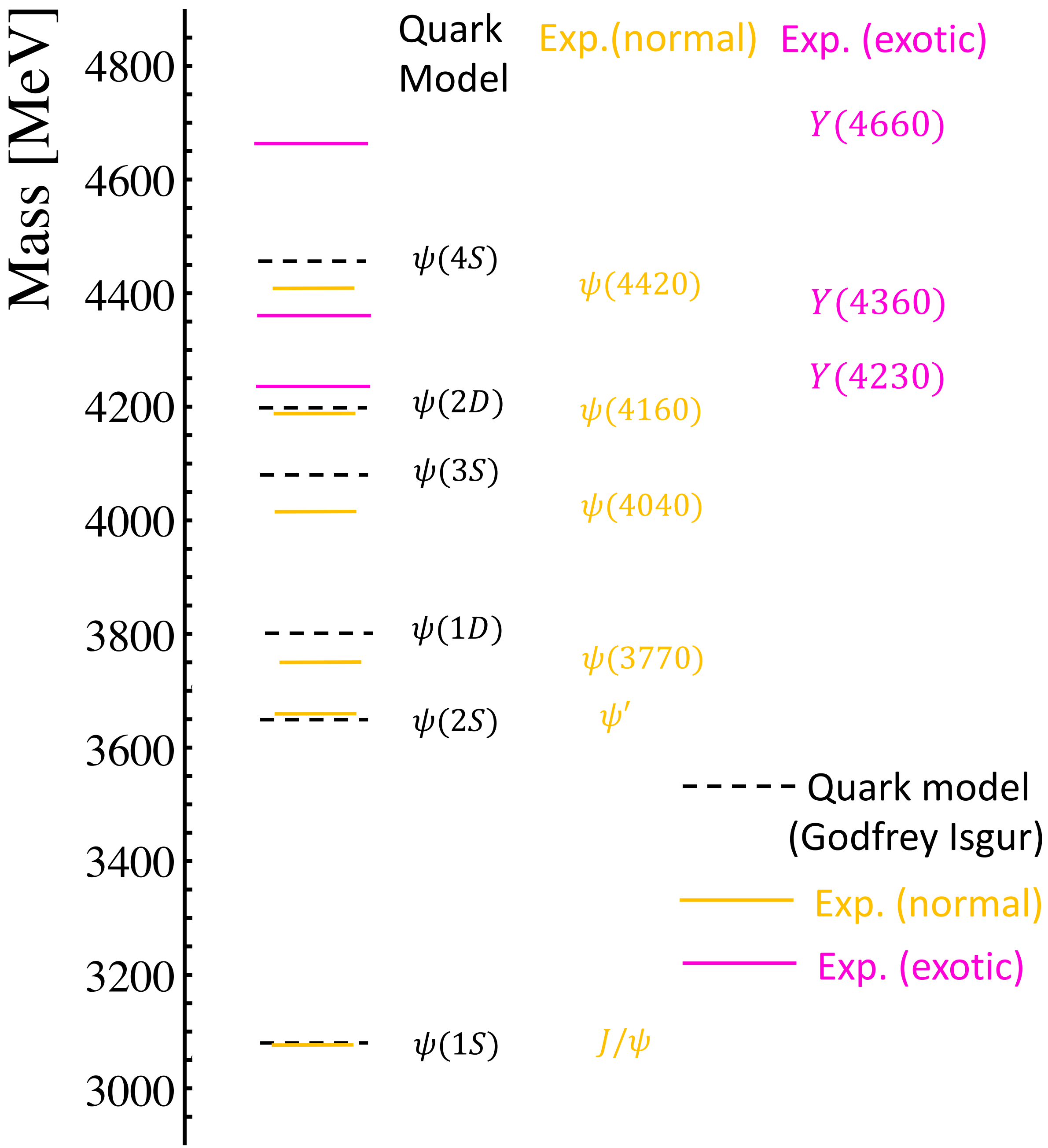

Reconsideration of quark model ?

Conventional method

Normal ψ masses → assigned to quark-model states (input)

→ quark-model parameters determined

Our analysis suggests:

- $\psi(4040)$ (conventionally assumed to be normal ψ) is mostly $D^*\bar{D}^*$ molecule
- $Y(4230)$ and $Y(4360)$ are mix of molecule (~60%) and $c\bar{c}$ (~40%)

No simple assignment of quark-model state to resonance

STCF would further request reconsideration of conventional wisdom

Summary

Summary

- Reviewed global coupled-channel analysis of $e^+e^- \to c\bar{c}$ data in $\sqrt{s} = 3.75 - 4.7$ GeV
- Reasonable fits overall
- Vector charmonium poles extracted

  -- All PDG states found

  -- Several more states near open-charm thresholds
- Compositeness calculated → many hadron-molecule-dominated states identified, including ψ(4040)

STCF significantly boosts coupled-channel analysis

- Higher $\sqrt{s}$ → discovery potential of heavier (vector) charmonium states
- Higher $\mathcal{L}$ → more precise and detailed data (Dalitz plots at each $\sqrt{s}$, etc.)

  -- more precise vector charmonium poles and residues (statistical improvement)

  -- less model-dependent charmonium poles and residues (systematics improvement)

Back up

Y width problem

Why Y states seem to have different widths for different final states ?

$\Gamma_{Y(4220)}$ ~ 44±4 MeV

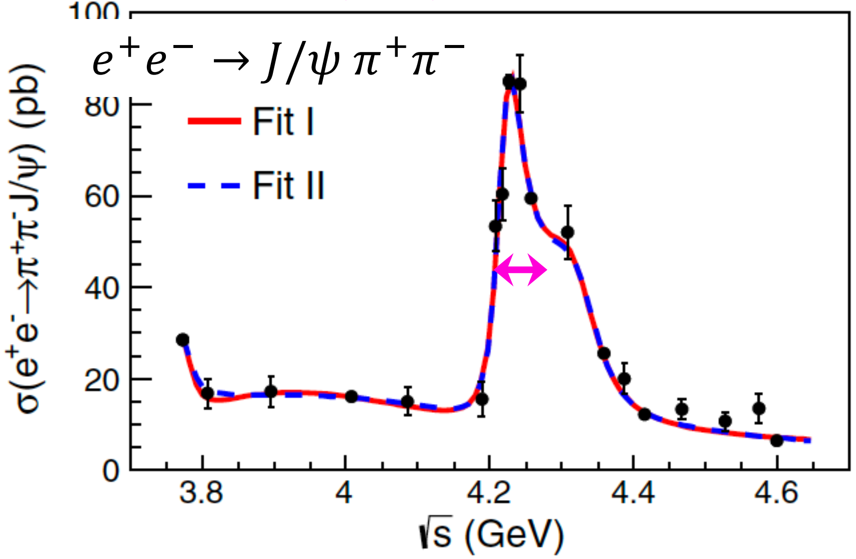

$\Gamma_{Y(4220)}$ ~ 77±7 MeV

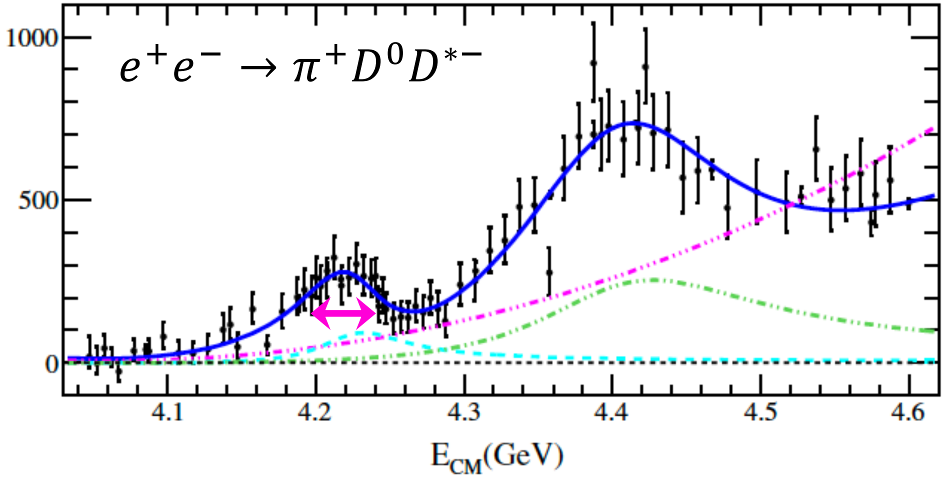

$\Gamma_{Y(4220)}$ ~ 82±6 MeV

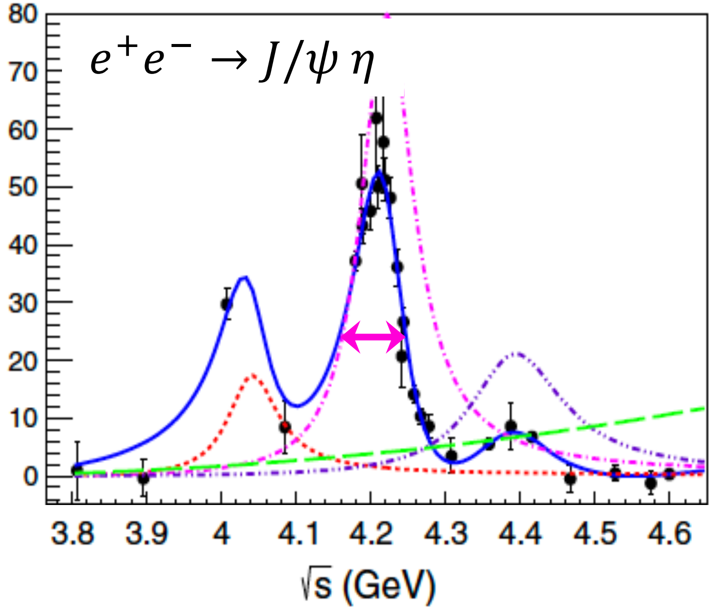

Y width problem revealed limitation of single-channel analysis

Single-channel analysis: analyze different final states with different models (usual experimental analysis)

Interference among overlapping resonances and non-resonant contributions is process dependent

→ Process dependent line-shape

Single-channel fits give process-dependent resonance parameters

→ Y width problem created

Y-width problem is artifact of single-channel analysis

Coupled-channel analysis

Analyze different final states simultaneously with a unified and (semi-)unitary model

Describe different lineshapes in different final states due to:

- Interference between various charmonium states and non-resonant amplitude
- Kinematical effects (threshold opening, triangle singularity)

Coupled-channel analysis clarifies how process-dependent Y lineshapes come about

At the same time, the analysis determines:

(i) vector charmonium mass, width (poles)

(ii) couplings of the poles with decay channels (residues)

Prerequisite to studying this

More outcomes from coupled-channel analysis

(i) vector charmonium mass and width (poles)

(ii) couplings of the poles with decay channels (residues)

↓ Input for further calculations

- Compositeness: probability of finding hadron molecule components in resonance

→ quantity to identify hadron molecule states

Baru et al., PLB 586, 53 (2004)
Sekihara et al. PTEP 063D04 (2015)

- Branching ratios: mostly unknown for charmonia of M > 4 GeV

including well-established $\psi(4040)$, $\psi(4160)$, $\psi(4415)$

Not straightforward, prescription needed

Heuser et al., EPJC 84, 599 (2024)

Understanding Y inevitably involves understanding Zc

Zc(3900), Zc(4020) : outstanding exotic candidates including $c\bar{c}u\bar{d}$

$e^+e^- \to J/\psi\,\pi^+\pi^-$ at Y(4220) region →

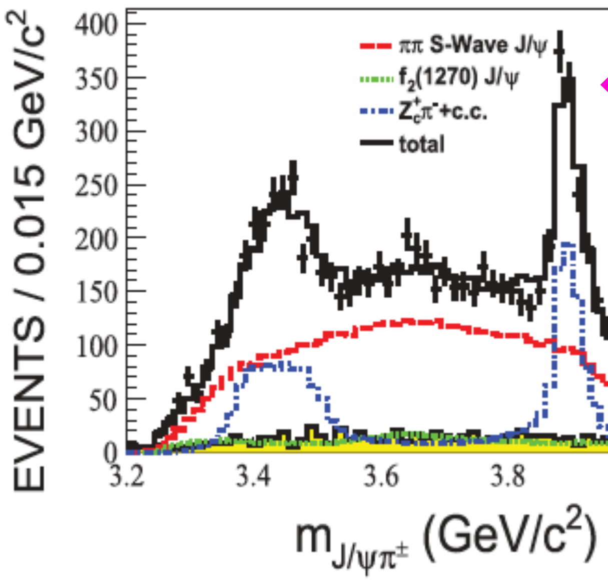

← Zc(3900)

Zc appears as:

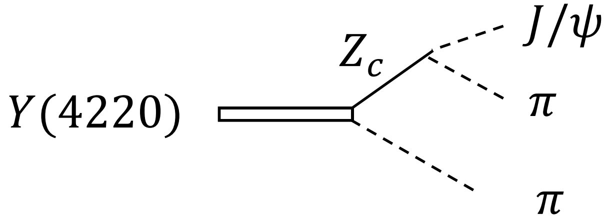

→ Y and Zc properties should be highly correlated

Global $e^+e^- \to c\bar{c}$ analysis consider Zc signals → address Y and Zc properties simultaneously

Related works previously done

Three-body model

* M. Cleven, Q. Wang, F.-K. Guo, C. Hanhart, U.-G. Meißner, Q. Zhao, PRD 90, 074039 (2014)

Analysis of $e^+e^- \to \pi D\bar{D}^*$, $J/\psi\pi\pi$, $h_c\pi\pi$ cross section and invariant mass in $4.1 \lesssim \sqrt{s} \lesssim 4.3$ GeV [Y(4230) region]

Pioneering works, but the data were very limited → limited conclusions on Y(4230) properties

* L. Detten, C. Hanhart, V. Baru, arXiv:2309.11970

Fitting data in Y(4230) region; more final states than the above

Our analysis includes significantly more complete dataset

→ More reliable conclusion

Fits to cross section data for 3-4 processes

* D.-Y. Chen, X. Liu, T. Matsuki, Eur. Phys. J. C 78, 136 (2018)

Breit-Wigner fit to $e^+e^- \to \pi D\bar{D}^*$, $J/\psi\pi\pi$, $h_c\pi\pi$ cross sections → Y(4320) and Y(4390) not necessary

* Z.-Y. Zhou, C.-Y. Li, Z. Xiao, arXiv:2304.07052

Two-body unitary model fitted to $e^+e^- \to D^{(*)}\bar{D}^{(*)}$, $\pi D\bar{D}$ cross sections → ψ(4160) is Y(4230)

Coupled-channels

assumed to be molecule-dominant
→ not directly from ψ decay

(quasi) two-body channels included; $J^{PC} = 1^{--}$

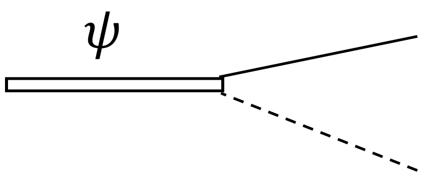

$f_0\, J/\psi,\ f_2\, J/\psi,\ f_0\, \psi',\ f_0\, h_c$

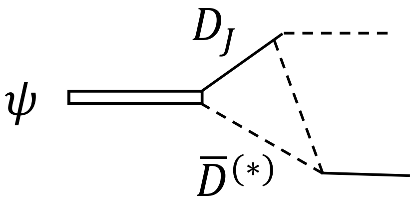

$D_0^*(2300)\bar{D}^*,\ Z_c\pi,\ Z_{cs}\bar{K}$

$D_0^*(2300), f_0, f_2, Z_c, Z_{cs}$ as (virtual) poles in two-body scattering amplitudes

$D\pi$ s-wave amplitude fitting LQCD-based amplitude

Albaladejo et al. PLB 767 (2017)

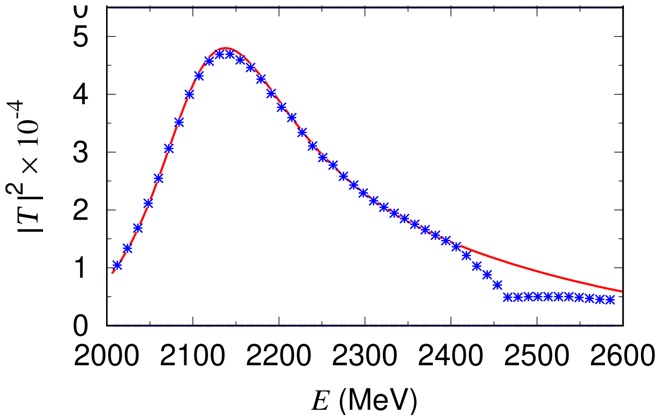

D_0^* pole :

2104 − i 100 MeV (ours)

$2105^{+6}_{-8} - i\ 102^{+10}_{-12}$ MeV
(Albaladejo et al.)

$\pi\pi - K\bar{K}$ s[d]-wave amplitude fitting empirical amplitude

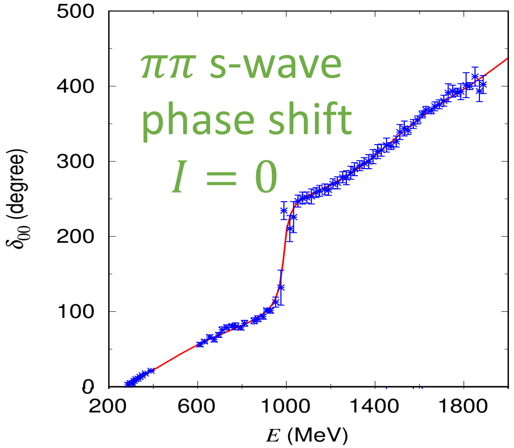

$\pi\pi$ s-wave
phase shift
$I = 0$

$f_0(500), f_0(980),$
$f_0(1370), f_2(1270)$ poles
→ consistent with PDG

$Z_{c(s)}$ amplitude

Z_c : $I\,J^{PC} = 1\;1^{+-}$ $\;D^*\bar{D} - D^*\bar{D}^* - J/\psi\pi - \psi'\pi - h_c\pi - \eta_c\rho$ couple—channel scattering amplitude

Z_{cs} : $I\,J^{P} = \frac{1}{2}\;1^{+}$ $\;D_s^*\bar{D} - D_s\bar{D}^* - J/\psi K$

driven by contact interactions; s-wave interactions except $h_c\pi$ p-wave interaction

$Z_{c(s)}$ amplitude

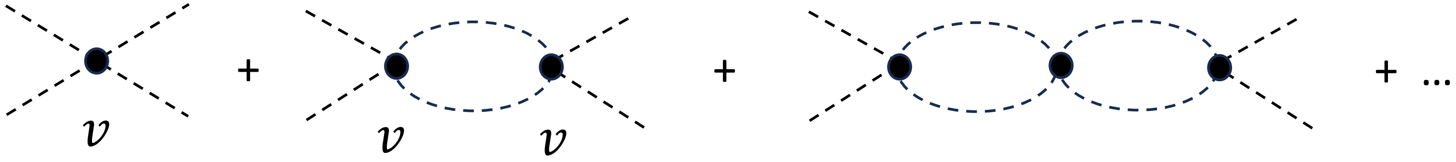

intermediate loops include

all possible coupled-channels

Assumptions

$v_{[D^*\bar{D}],[D^*\bar{D}]} = v_{D^*\bar{D}^*,D^*\bar{D}^*} = v_{[D_s^*\bar{D}],[D_s^*\bar{D}]}$ (HQSS, SU(3))

$v_{[D^*\bar{D}],J/\psi\pi} = v_{[D_s^*\bar{D}],J/\psi K}$ (SU(3))

$C = -1$ basis

$$[D^*\bar{D}] = \frac{1}{\sqrt{2}}(D^*\bar{D} - D\bar{D}^*)$$

$$[D_s^*\bar{D}] = \frac{1}{\sqrt{2}}(D_s^*\bar{D} - D_s\bar{D}^*)$$

SU(3)

no coupling between hidden-charm channels (e.g. $v_{J/\psi\pi,J/\psi\pi} = v_{J/\psi\pi,\psi'\pi} = 0$)

Nonzero couplings are determined by the global fit → poles may be generated if required by data

Short-range mechanisms among open-charm channels

example

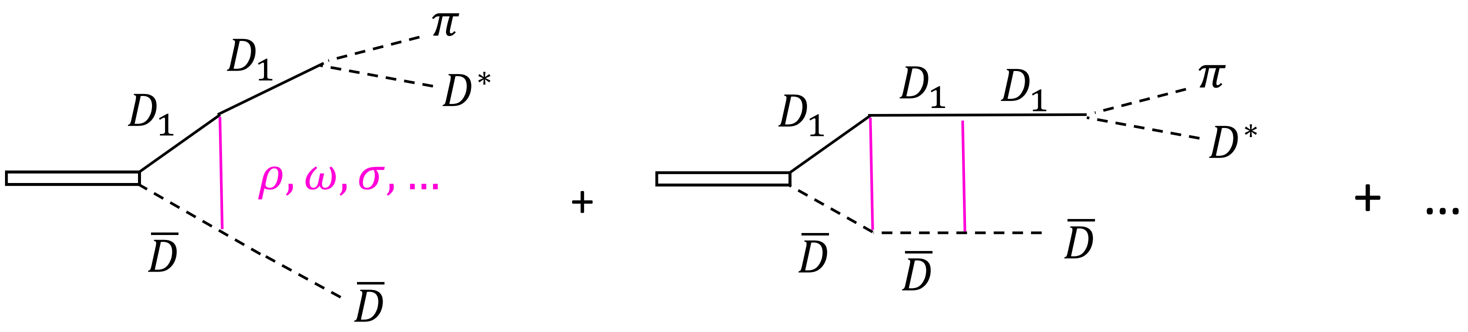

G.-J. Ding, PRD 79, 014001 (2009)
X.-K. Dong et al., PRD 101, 076003 (2020)

→ $D_1\bar{D}$, $D_1\bar{D}^*$ molecule states

Y(4220) Y(4360)

simulate

→

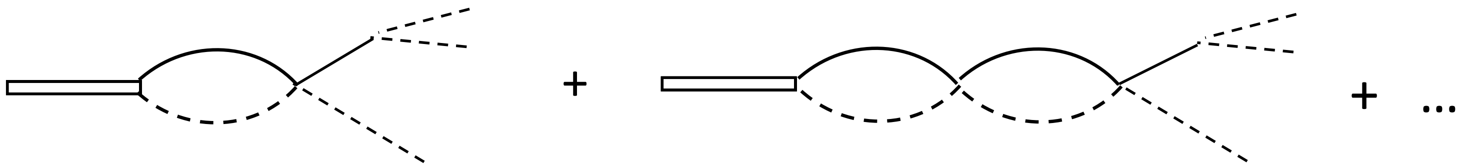

(Our model)

Contact interactions among $D_1\bar{D}^{(*)}$, $D_2^*\bar{D}^*$, $D^{(*)}\bar{D}^{(*)}$, $D_{s1}\bar{D}_s$, $D_s^{(*)}\bar{D}_s^{(*)}$, $\Lambda_c\bar{\Lambda}_c$ channels

→ fitted to data (advantage of separable interactions)

- High-precision BESIII data require these contributions (enhanced threshold cusps)
- Potentially generate hadron-molecule states

Global analysis can examine if Y(4220) as $D_1\bar{D}$ molecule and Y(4360) as $D_1\bar{D}^*$ molecule

ψ production mechanisms

$e^+e^- \to c\bar{c}$ data in $3.75 \leq \sqrt{s} \leq 4.7$ GeV region → Charmonium excitations are important mechanism

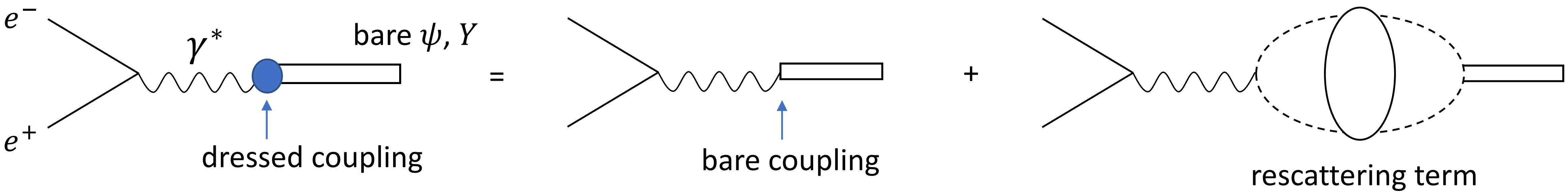

Data determine how many bare states to be included (5 bare states) and which charmonium states exist

Expected states $\psi(3770)$, $\psi(4040)$, $\psi(4160)$, $\psi(4415)$, $Y(4220)$, $Y(4360)$

Data is not sufficient for coupled-channel analysis in $\sqrt{s} > 4.6$ GeV (three-body final states including $c\bar{c}s\bar{s}$)

→ $Y(4660)$ is not included in coupled-channel amplitude → included as a Breit-Wigner amplitude

Three-body decays of ψ

$e^+e^- \to \pi D^*\bar{D}$

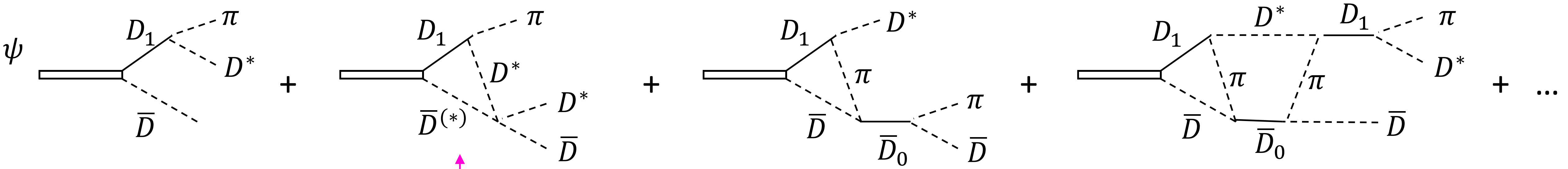

(until infinite loops)

$e^+e^- \to J/\psi\pi\pi$

Triangle singularity loop

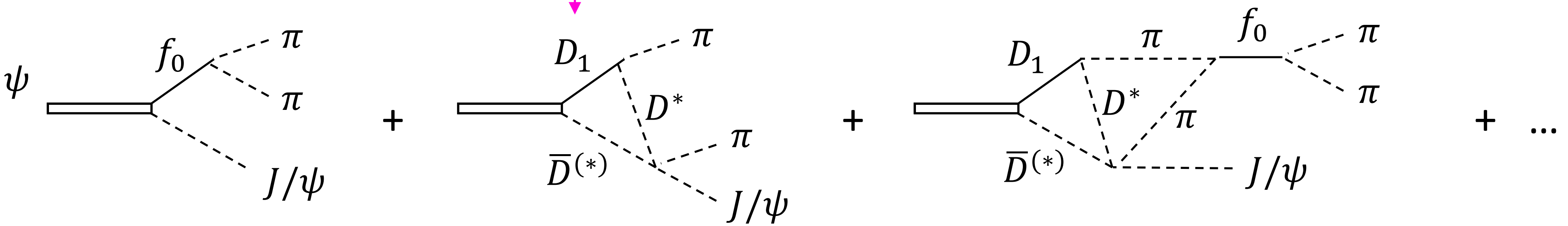

(until infinite loops)

Selected important diagrams; diagrams with more loops are usually more suppressed

Different processes share the same interactions ← unitarity requirement

$e^+e^- \to \pi D^*\bar{D}$

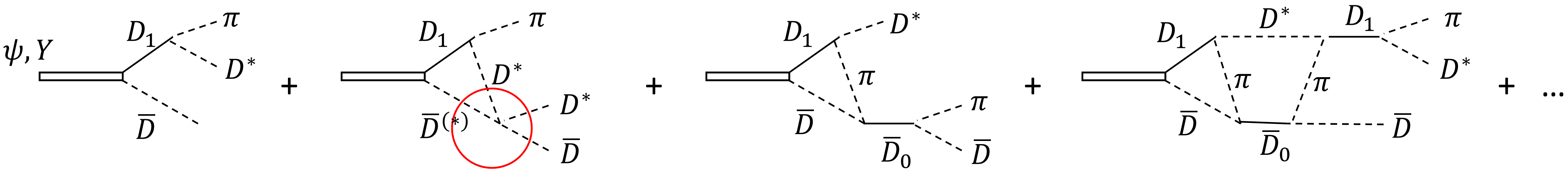

(until infinite loops)

$e^+e^- \to J/\psi\pi\pi$

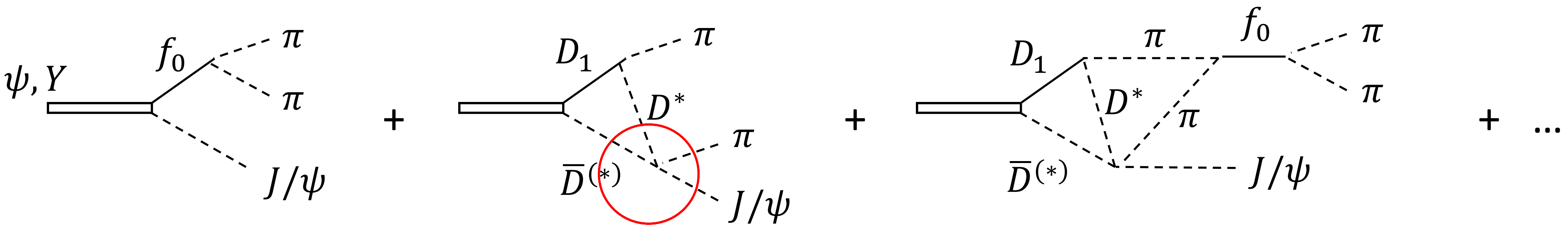

(until infinite loops)

Z_c amplitude

$D^*\bar{D} - D^*\bar{D}^* - J/\psi\,\pi - \psi'\pi - h_c\pi - \eta_c\rho$ coupled-channel scattering amplitude ($J^{PC} = 1^{+-}$)

→ $D^*\bar{D}$ and $D^*\bar{D}^*$ threshold cusps will be created in invariant mass distributions

Zc(3900) and Zc(4020) poles may also be generated (if needed by data) to enhance the cusps

Fitting parameters in global analysis

* bare ψ masses (5 bare states)

* bare ψ coupling constants (real)

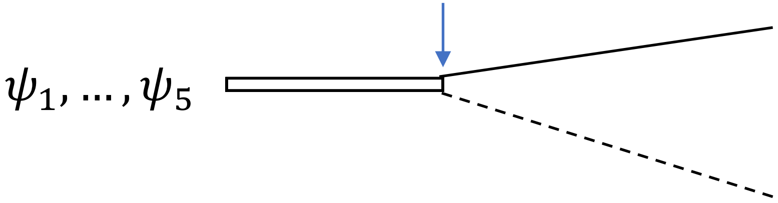

* bare photon-ψ coupling constants (real)

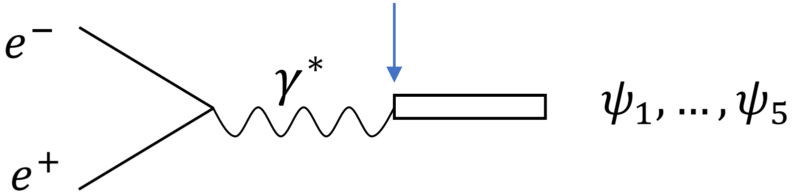

* non-resonant photon coupling constants (real)

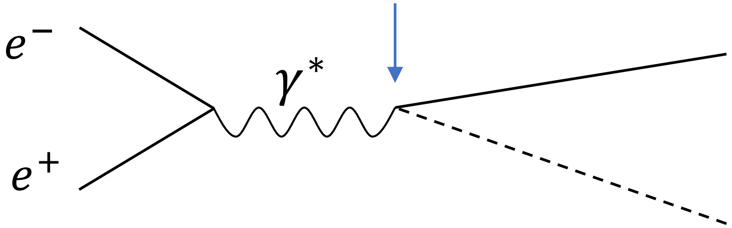

* $\psi(4660)$, $\psi(4710)$ Breit-Wigner mass, width, vertices

* coupling constants in Z_c amplitude :

$v_{D^*\bar{D},D^*\bar{D}}$, $v_{D^*\bar{D},J/\psi\pi}$, $v_{D^*\bar{D},\psi'\pi}$ etc.

* Contact-interaction strengths among open-charm channels

* Cutoffs in non-resonant vertices for

$$\gamma^* \to D^{(*)}\bar{D}^{(*)}, D_s^{(*)}\bar{D}_s^{(*)}, \Lambda_c\bar{\Lambda}_c$$

In total, 200 fitting parameters

$$\chi^2/\text{ndf} = 2320/(1635 - 200) \sim 1.6$$

$e^+e^- \to \psi' \pi^+\pi^-$

Data: BESIII, PRD 104, 052012 (2021)

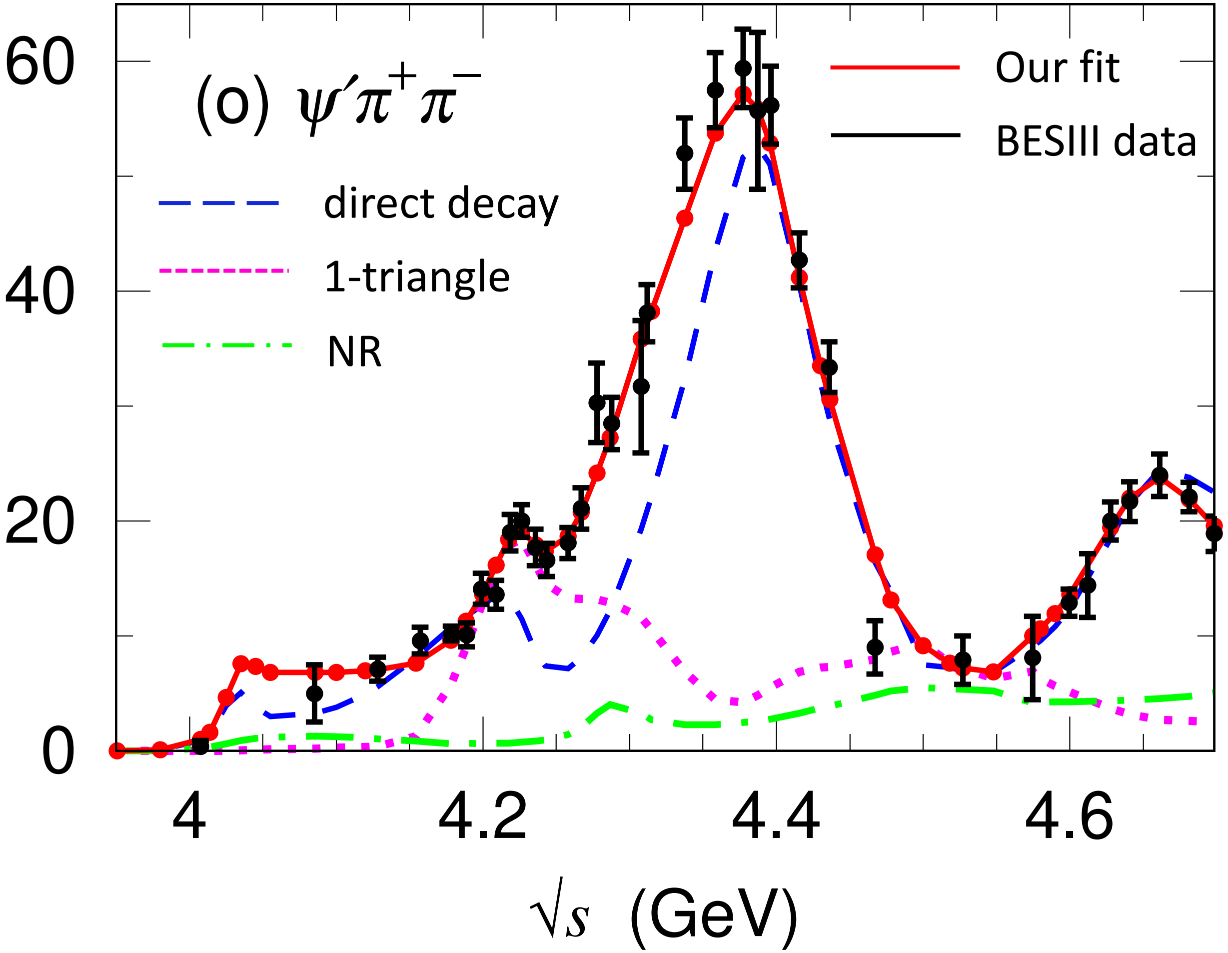

- Overall good fit
- Enhancement at ~ 4.03 GeV is from $\psi(4040)$

  ← consequence of coupled-channel fit
- 1-triangle contribution is large at $\psi(4220)$ peak

$e^+e^- \to \psi' \pi^+\pi^-$

Fit to $\psi'\pi$ invariant mass distributions

Data: BESIII, PRD 96, 032004 (2017)

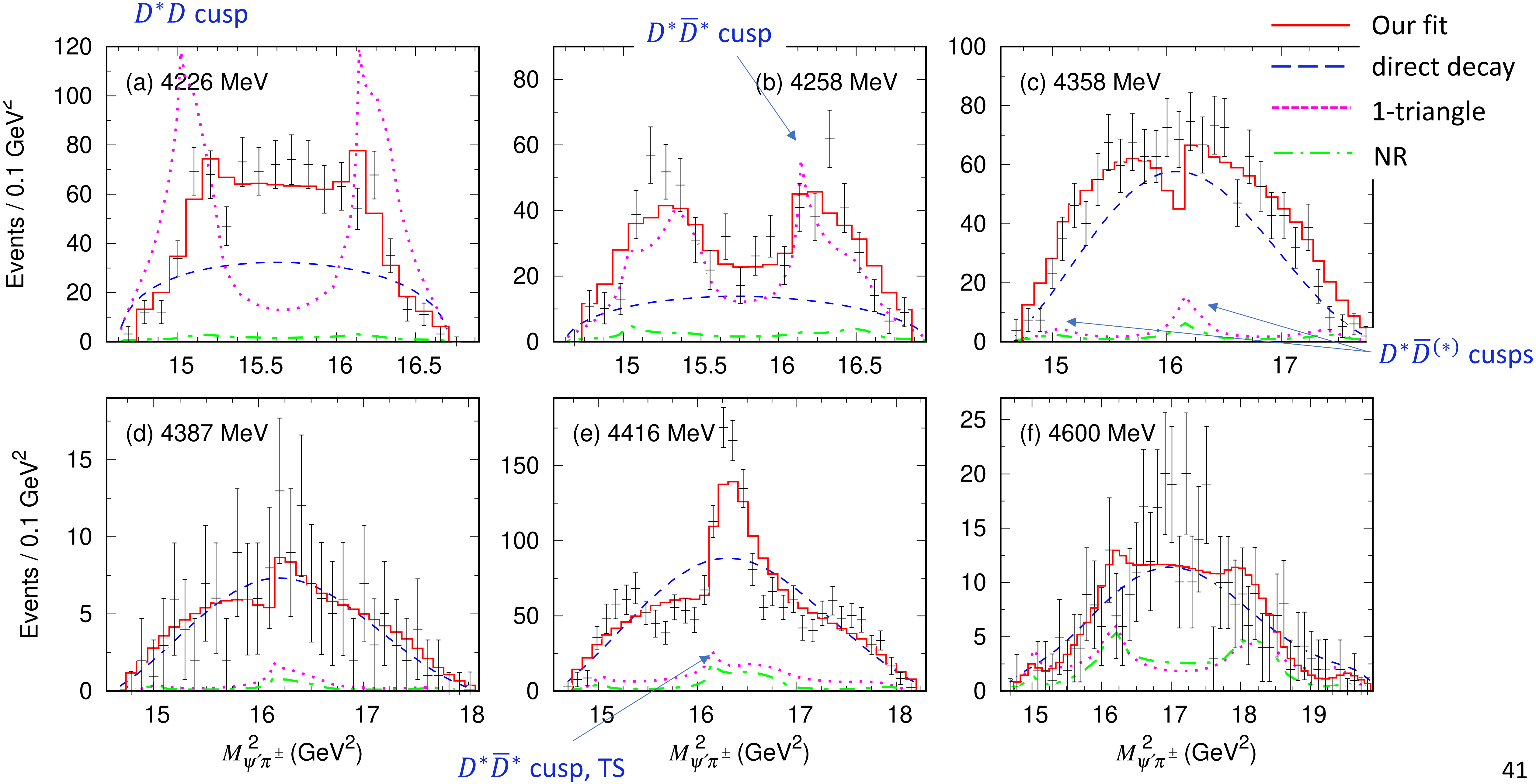

$e^+e^- \to \psi' \pi^+\pi^-$

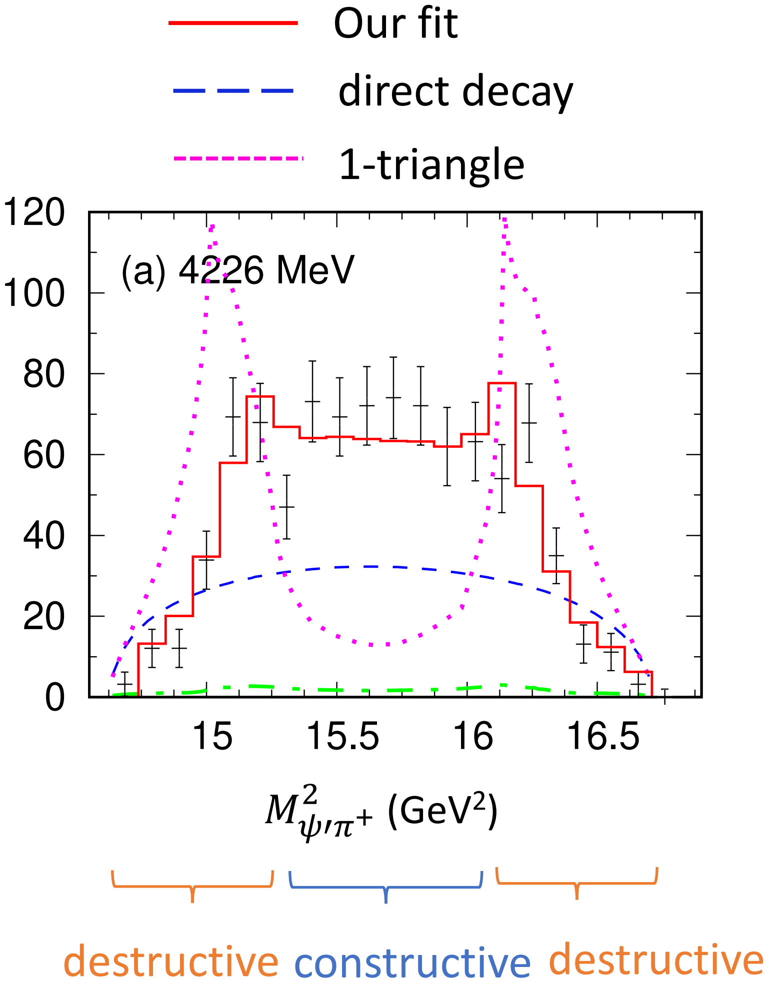

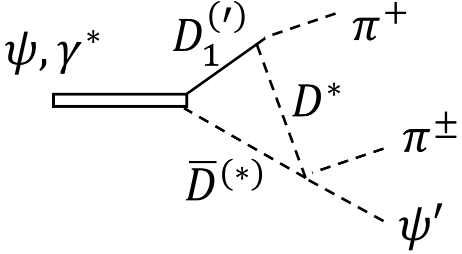

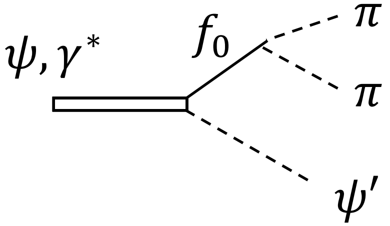

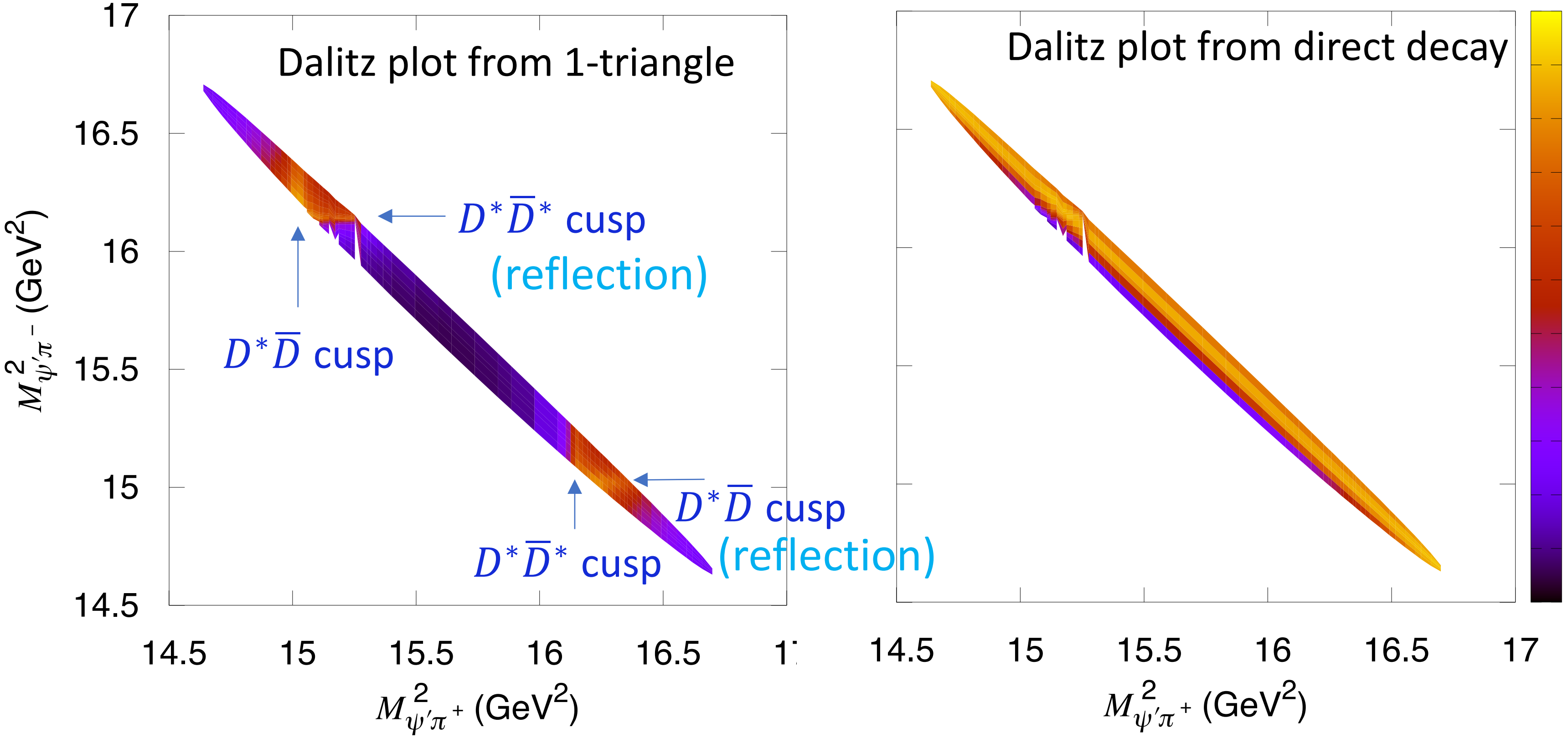

Interference erase cusp structures

$e^+e^- \to \psi' \pi^+\pi^-$

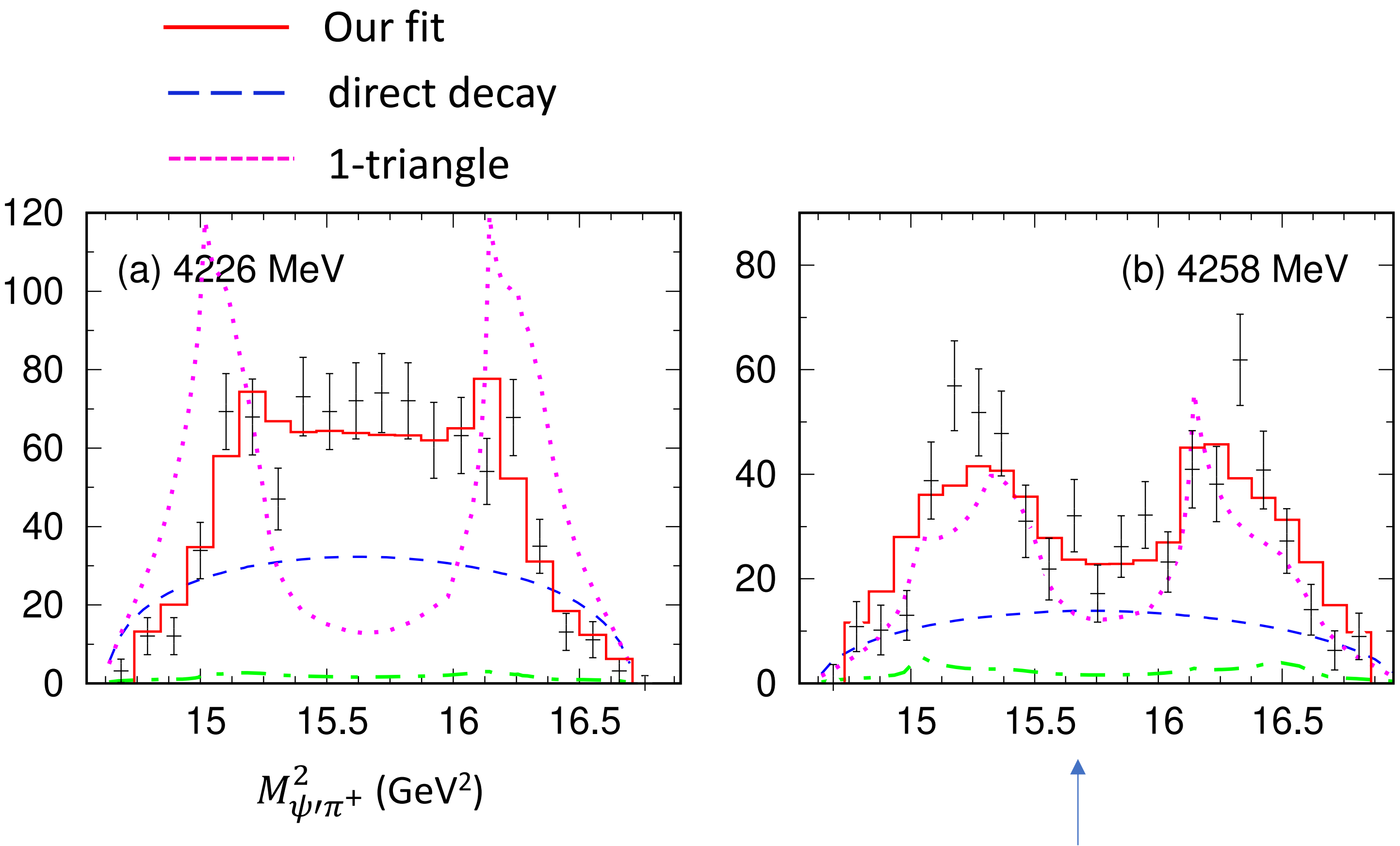

destructive constructive destructive

Interference erase cusp structures

direct-decay contribution smaller

→ Smaller interference

→ Clearer cusp structures

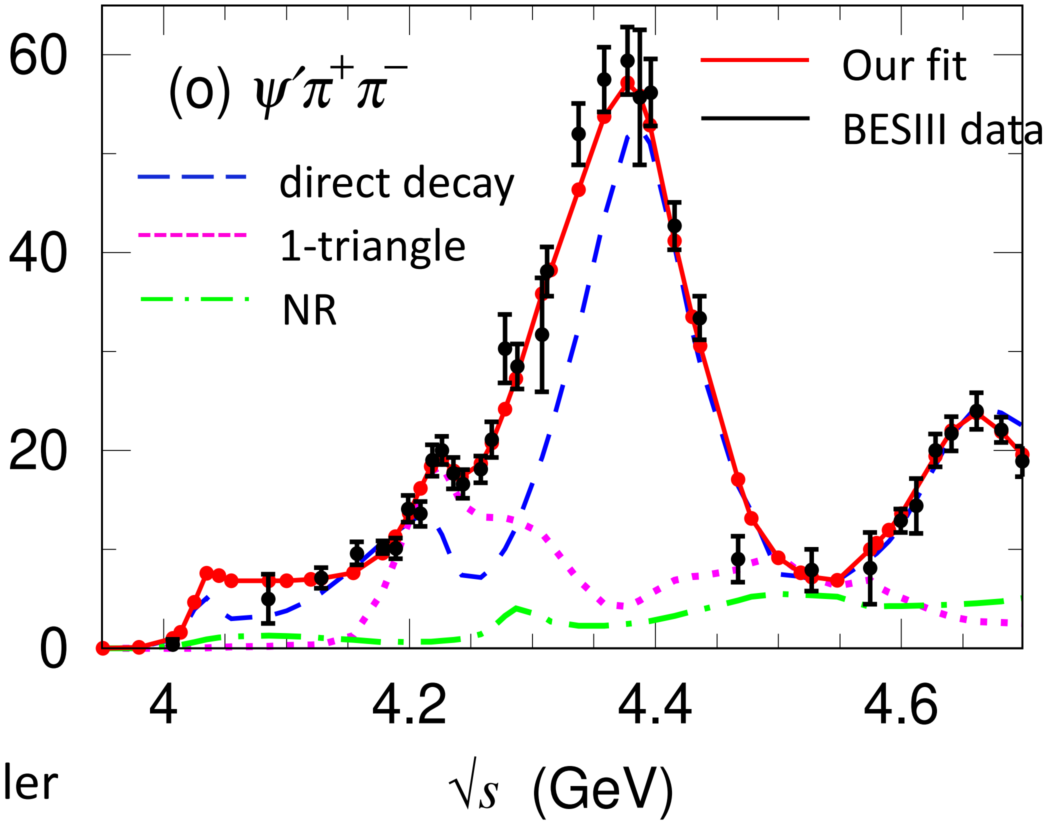

First explanation of this rapid change of lineshape

$e^+e^- \to D^{(*)}\bar{D}^{(*)}$

Data: BESIII, PRL 133, 081901 (2024)
JHEP 05 (2022) 155.
Belle, PRD 97, 012002 (2018)

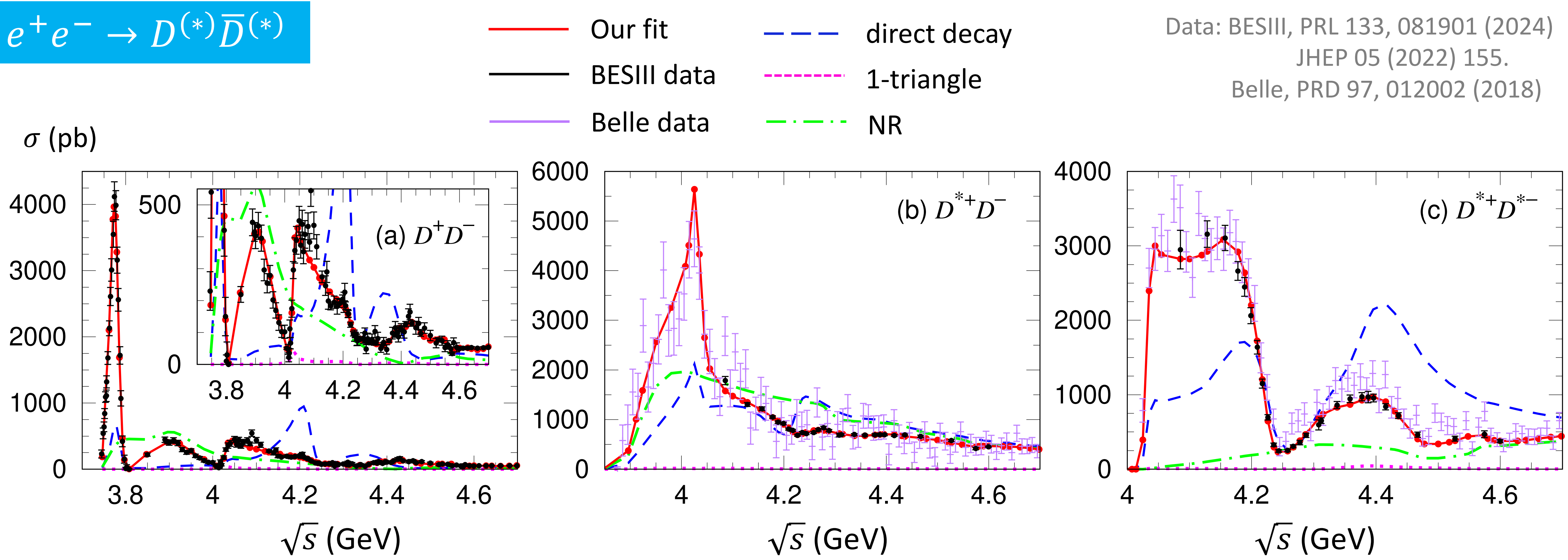

- *Precise* BESIII data are well fitted
- Contact interactions among open-charm channels important (difference between blue and red curves above)
- 1-triangle (particle exchange) is small

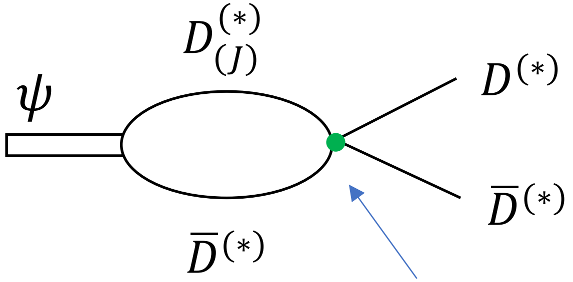

Open-charm rescattering by short-range interactions

→ molecule formation

$e^+e^- \to D^{(*)}\bar{D}^{(*)}$

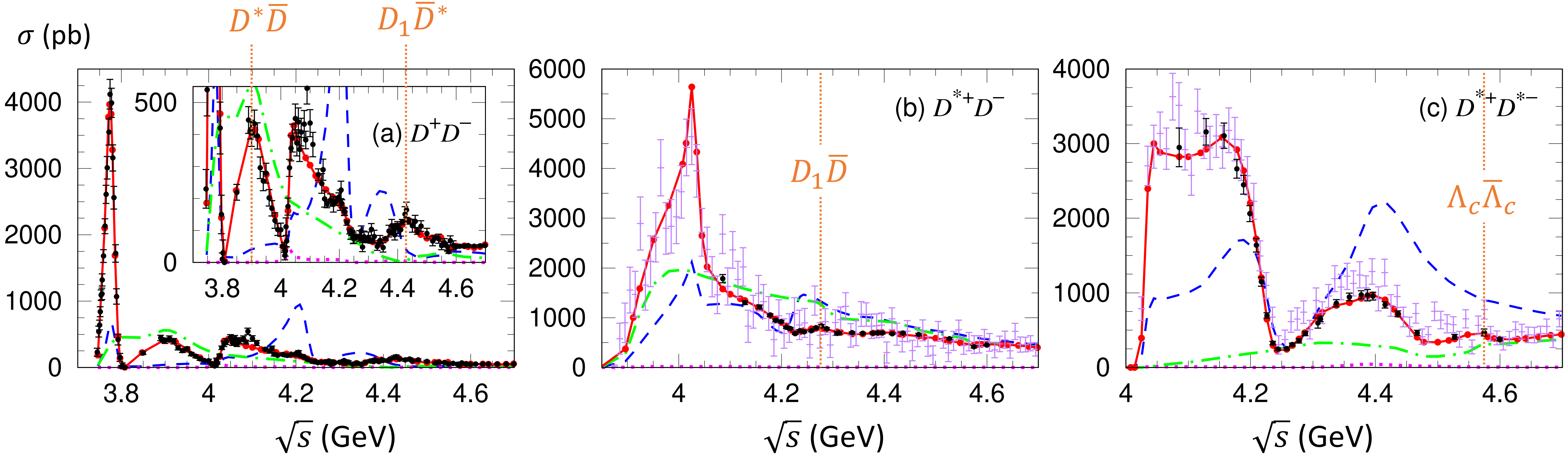

Fitting precise data, we need threshold cusps from

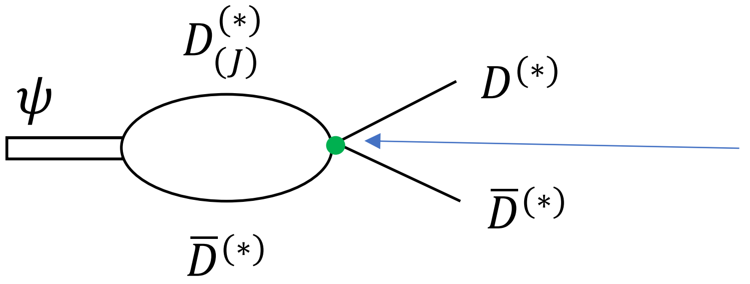

Open-charm rescattering
by short-range interactions

Fitting cusps → good constraints on interactions among open-charm channels

→ good constraints on existence of $D_{(J)}^{(*)}\bar{D}^{(*)}$ molecules

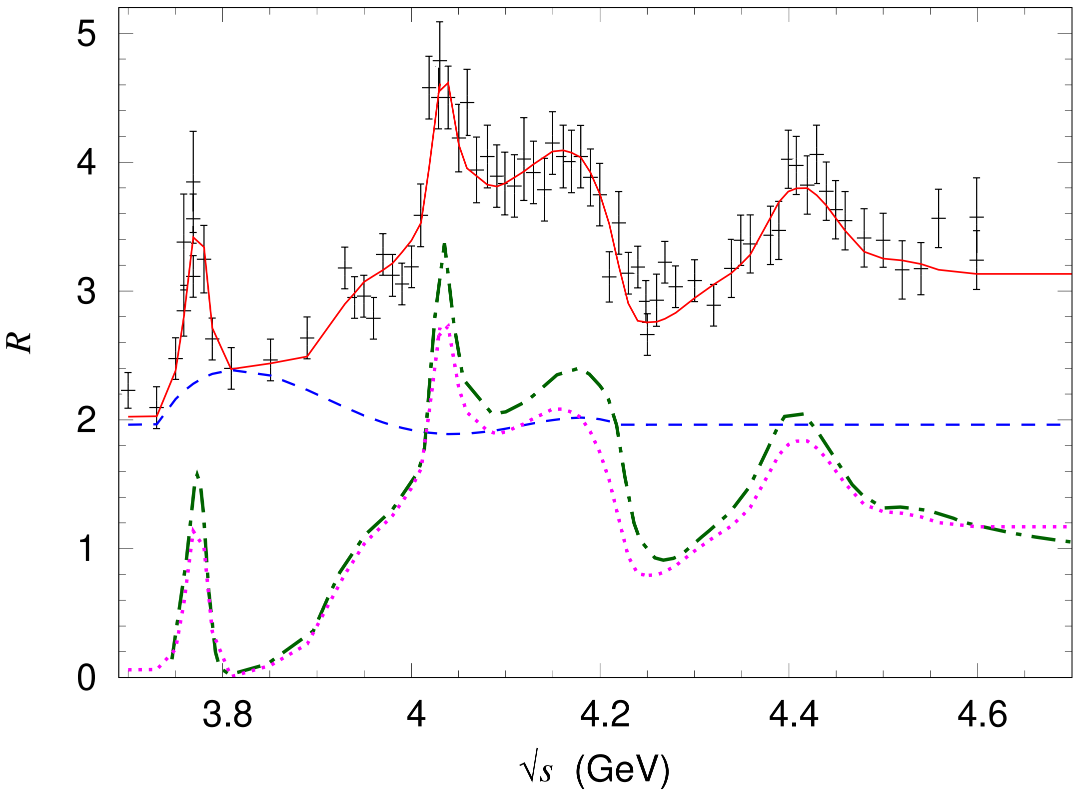

$$
\begin{aligned}
R(s) &= \frac{\sigma(e^+e^- \to \text{hadrons})}{\sigma^{\text{tree}}_{e^+e^-\to\mu^+\mu^-}(s)} \\
&= R_c(s) + R_{uds}(s),
\end{aligned}
$$

Vacuum polarization $\Pi_c =$

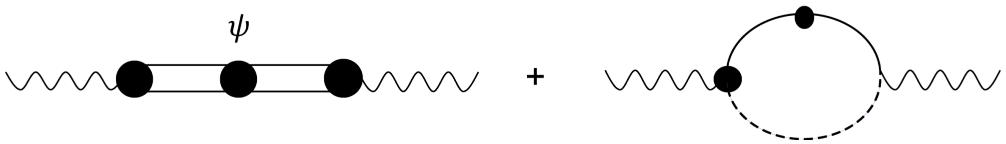

Optical theorem $R_c(s) = -\dfrac{3}{\alpha}\mathrm{Im}[\Pi_c(s)],$ (green dash-dotted curve)

$e^+e^- \to \mu^+\mu^-$ cross section prediction

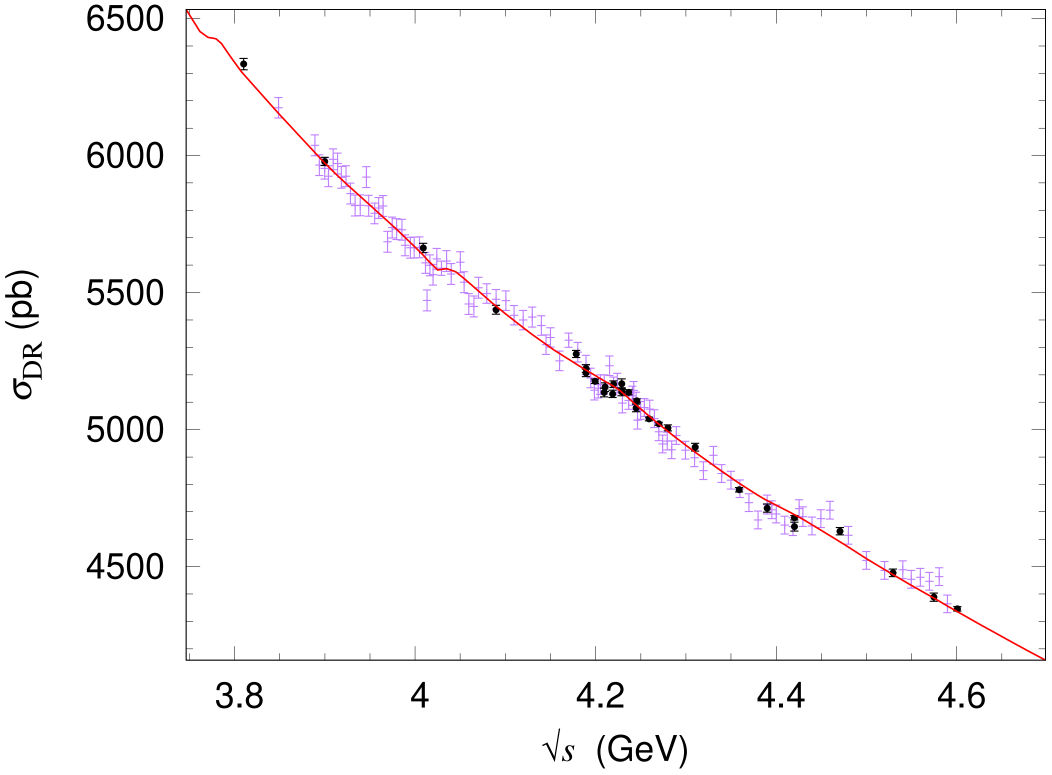

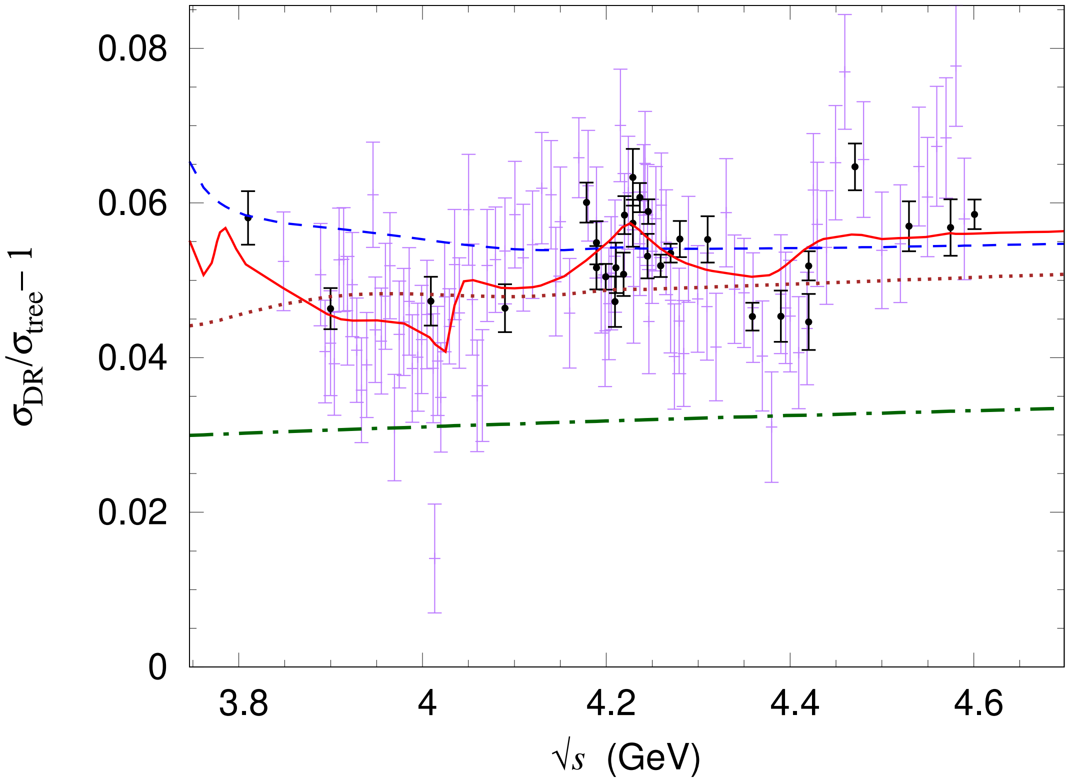

$$\sigma^{\rm DR}_{e^+e^-\to\mu^+\mu^-}(s) = \sigma^{\rm tree}_{e^+e^-\to\mu^+\mu^-}\,(1 + 2{\rm Re}[\Pi(s)])$$

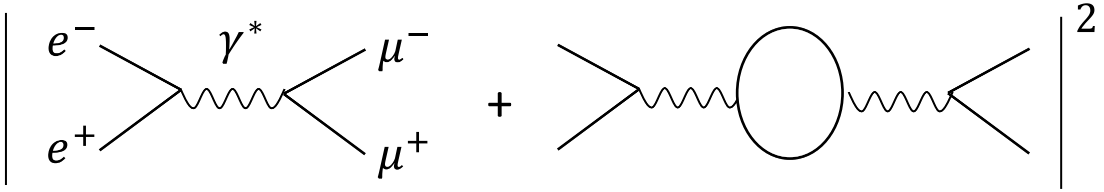

$$\Pi(s) = \Pi_{\rm lepton} + \Pi_{uds} + \Pi_{J/\psi} + \Pi_{\psi'} + \Pi_c$$

Zc poles

from $J^{PC}=1^{+-}$ $D^*\overline{D}-D^*\overline{D}^*-J/\psi\pi-\psi'\pi-h_c\pi-\eta_c\rho$ couple—channel amplitude

$E_{Z_c}^{\text{This work}}$	$M_{Z_c}^{\text{PDG}}$	$\Gamma_{Z_c}^{\text{PDG}}$	
$(3837.7\pm7.4)+(19.4\pm1.6)i$	3887.1 ± 2.6	28.4 ± 2.6	$Z_c(3900)$
$(3989.9\pm5.6)+(26.1\pm4.3)i$	4024.1 ± 1.9	13 ± 5	$Z_c(4020)$

$D^*\overline{D}$, $D^*\overline{D}^*$ virtual poles
(below thresholds)

Zc(3900) pole: comparison with LQCD result

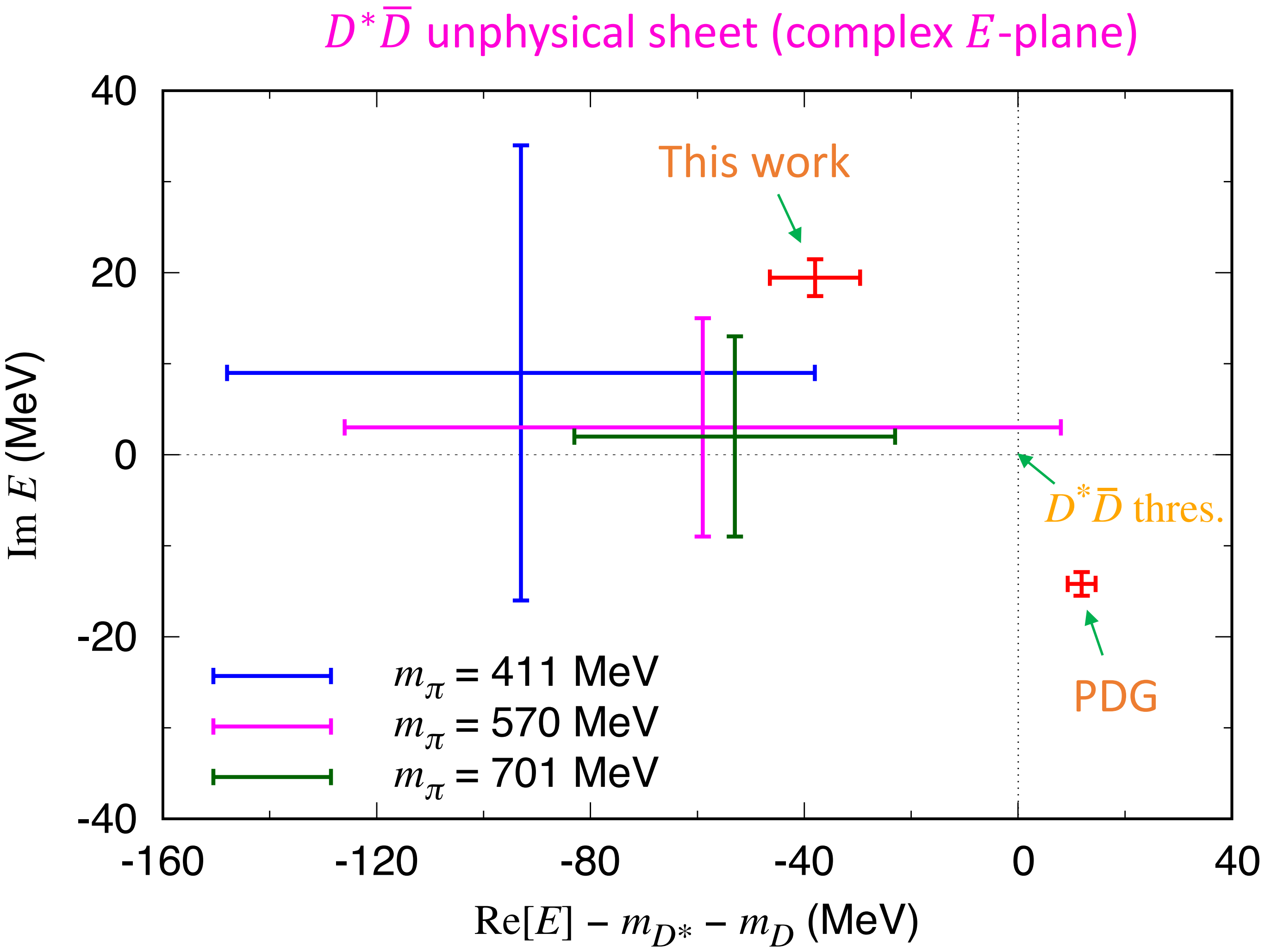

LQCD ($m_\pi = 411$ MeV)
HAL QCD, J. Phys. G 45, 024002 (2018)

$m_{D^*} + m_D - (93 \pm 55 \pm 21) + (9 \pm 25 \pm 7)i$ MeV

$S(\{-k_i^*\}) = S^*(\{k_i\})$ applied; PRD 105, 014034 (2022)

This work

$m_{D^*} + m_D - (38 \pm 7.4) + (19 \pm 1.6)i$ MeV

PDG

$m_{D^*} + m_D + (11.9 \pm 2.6) - (14.2 \pm 1.3)i$ MeV

LQCD and this work are fairly consistent (virtual poles)

Zc(3900) pole: virtual or resonance

In literature, various models are used to describe Zc(3900)

→ fit $J/\psi\pi$ and $D^*\overline{D}$ invariant mass distributions, NOT cross-section data

→ either virtual or resonance solutions How to discriminate ?

Searching Zc-resonance solution

energy-dependent $D^*\overline{D}^{(*)}$ interactions in default-fit model → refit all parameters for global fit → $\chi^2 \sim 2510$

→ not comparable to the default model with χ^2 = 2320 (Zc-virtual solution)

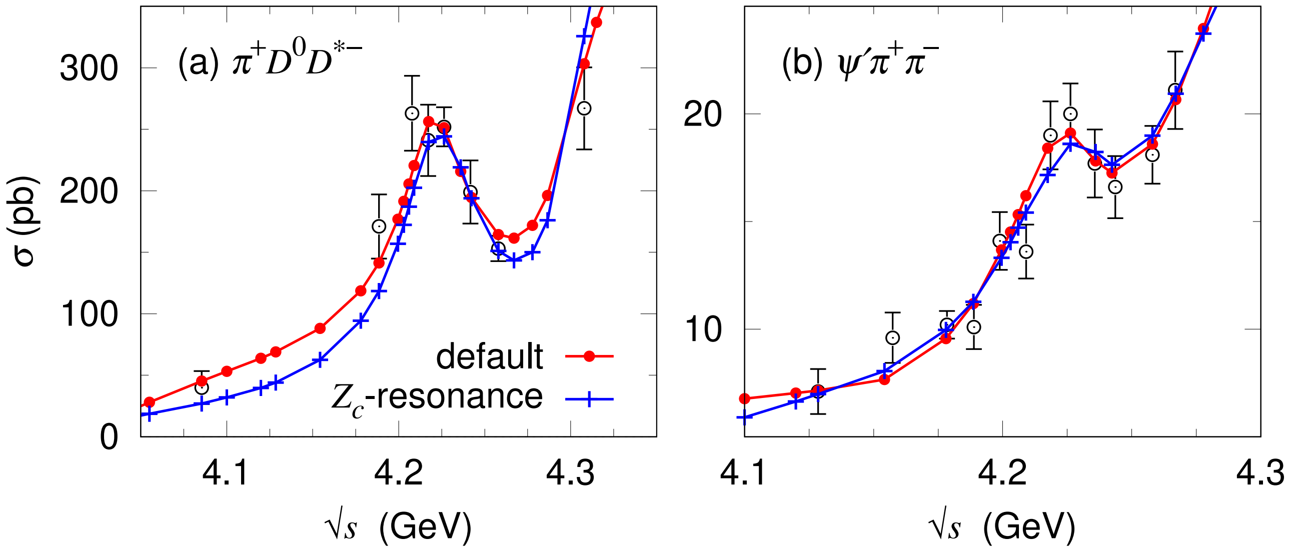

Suggestion:

Fitting cross section data may discriminate

Zc pole location

ψ poles from their dressed propagator

(we are not using BW)

Full amplitude

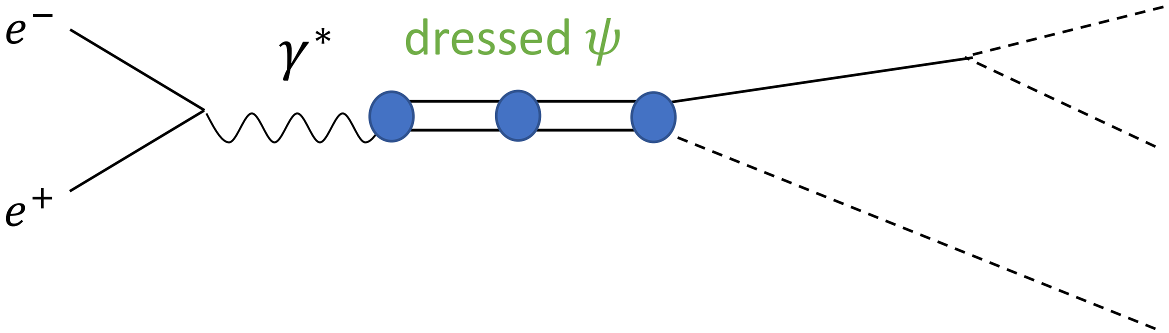

+ non-resonant

dressed ψ = $G_\psi(E)$

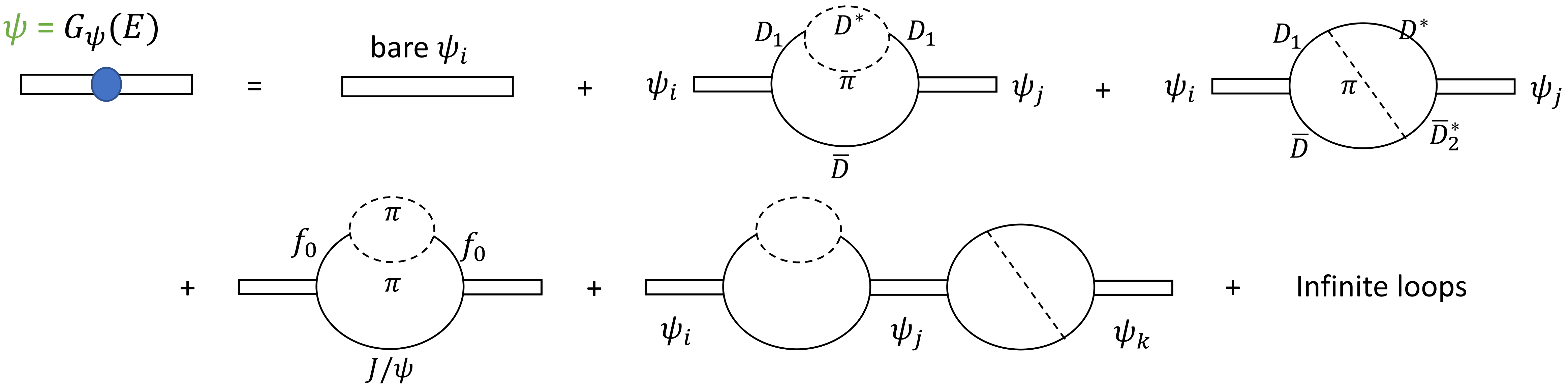

Search complex energy E_ψ where $G_\psi(E_\psi) = \infty$ (E_ψ: pole energy, pole position) by analytical continuation of $G_\psi(E)$

Resonance parameters

This work		PDG(ψ) [4], BESIII [16, 38, 88]		
M (MeV)	Γ (MeV)	M (MeV)	Γ (MeV)	
3764.2 ± 2.0	47.3 ± 2.6	3751.9 ± 3.8	32.8 ± 5.8	$\mathcal{R}(3760)$
3780.2 ± 1.2	29.9 ± 2.3	3778.1 ± 0.7	27.5 ± 0.9	$\psi(3770)$
3898.4 ± 0.9	127.5 ± 6.7	3872.5 ± 14.2	179.7 ± 14.1	$G(3900)$
3956.1 ± 1.0	96.8 ± 10.4	–	–	$^{\rm r}D_s\bar{D}_s$
4029.2 ± 0.4	26.3 ± 1.0	4039 ± 1	80 ± 10	$\psi(4040)$
4052.4 ± 0.4	49.0 ± 0.3	–	–	$^{\rm v}D_s^*\bar{D}_s$
4192.2 ± 2.2	129.3 ± 4.2	4191 ± 5	70 ± 10	$\psi(4160)$
4216.2 ± 0.5	40.3 ± 1.0	–	–	$^{\rm v}D_s^*\bar{D}_s^*$
4229.9 ± 0.9	46.4 ± 2.6	4222.5 ± 2.4	48 ± 8	$\psi(4230)$
4308.1 ± 2.2	138.2 ± 4.4	4298 ± 12	127 ± 17	$Y(4320)$
4346.2 ± 3.8	122.8 ± 6.7	4374 ± 7	118 ± 12	$\psi(4360)$
4390.1 ± 2.0	106.5 ± 4.1	4421 ± 4	62 ± 20	$\psi(4415)$
4496.3 ± 3.1	16.4 ± 2.1	–	–	$^{\rm b}D_{s1}\bar{D}_s$
4579.6 ± 1.7	-5.2 ± 7.6	–	–	$^{\rm b}\Lambda_c\bar{\Lambda}_c$
4655.9 ± 3.0	134.9 ± 5.9	4630 ± 6	72^{+14}_{-12}	$\psi(4660)$

← BW fit

$$M = \mathrm{Re}[E_\psi]$$

$$\Gamma = -2\times\mathrm{Im}[E_\psi]$$

No Y-width puzzle by construction:

same Y-widths for all final states

Hadron-molecule poles

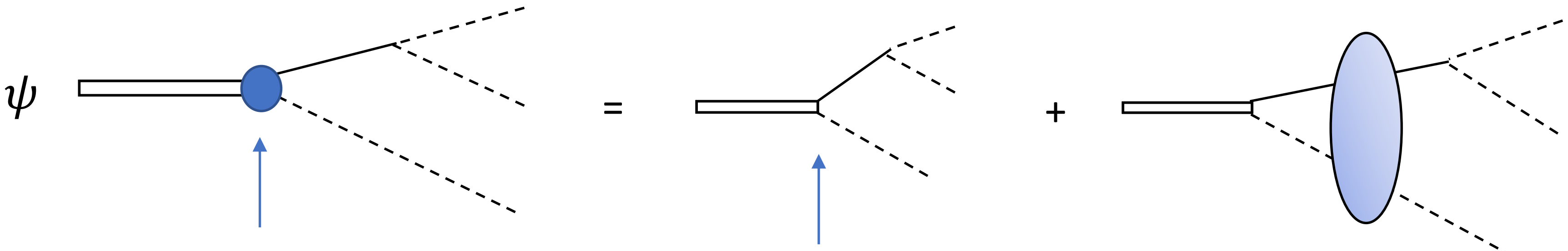

dressed decay vertex

bare vertex

rescattering terms (final-state interactions)

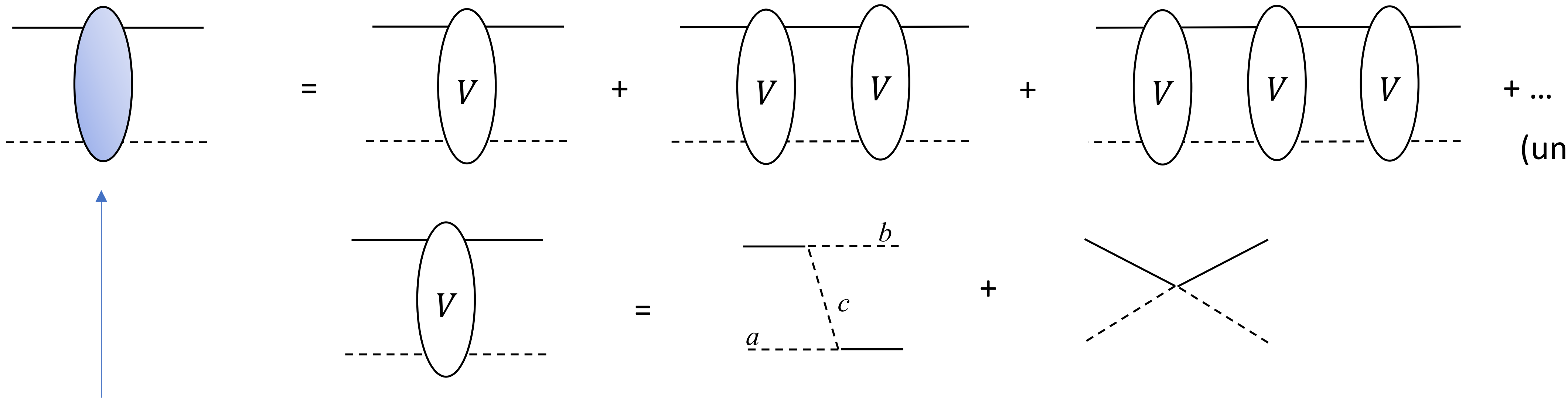

(until infinite loops)

This amplitude may include hadron-molecule poles

$$\propto \frac{1}{E - E_a - E_b - E_c}$$

E-independent

Pole locations (no coupling to bare ψ)

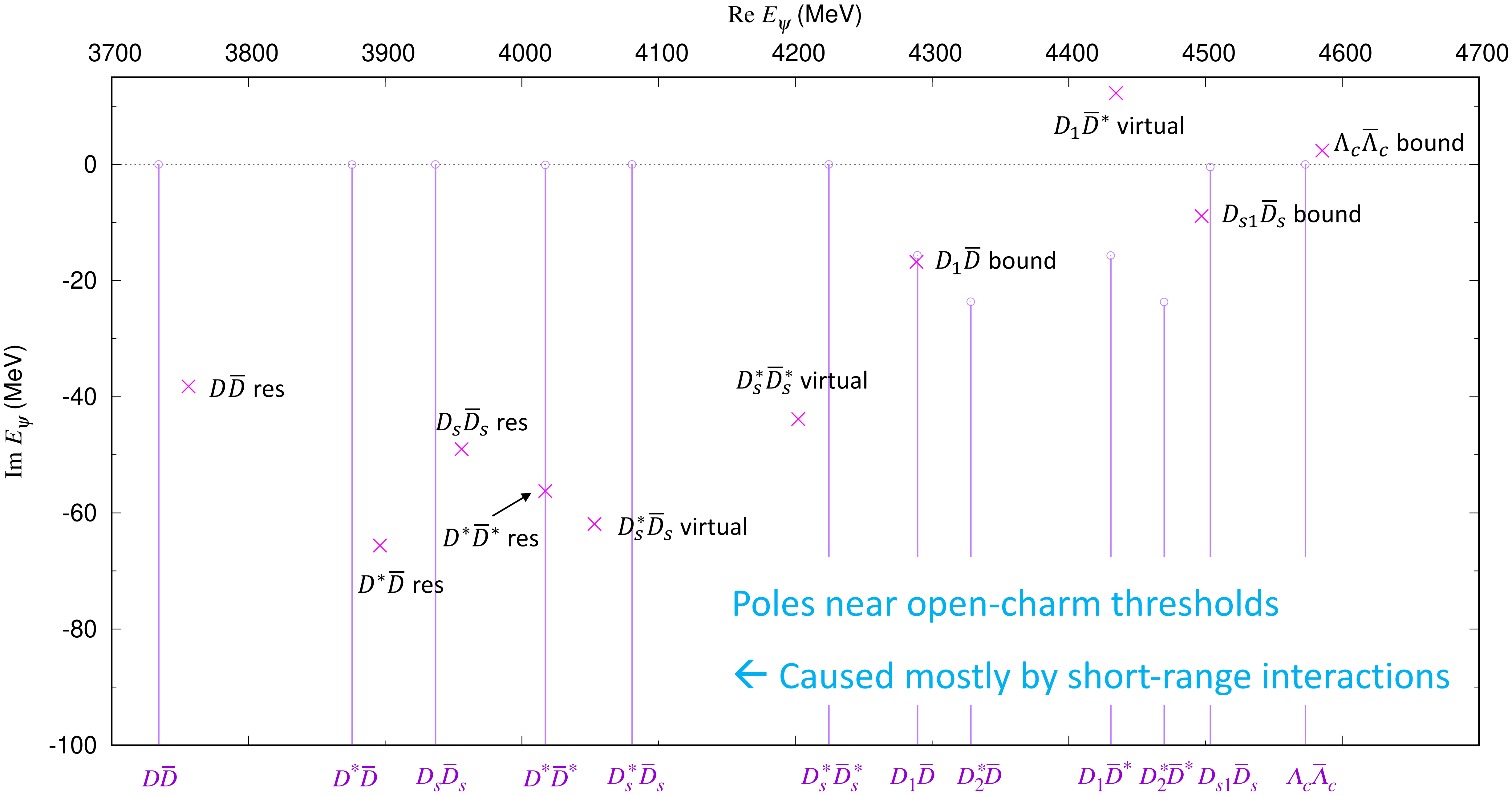

Poles near open-charm thresholds

← Caused mostly by short-range interactions

Compositeness

T. Sekihara et al., PTEP 2015 (2015) 063D04

Normalization of resonance (Gamow) state $(\psi|\psi) = 1$ $\quad H\,|\psi) = \left(M - i\,\frac{\Gamma}{2}\right)|\psi)$

Insert complete set

$$1 = \sum_{a} |\psi_a\rangle\langle\psi_a| + \sum_{j} \int \frac{d^3q}{(2\pi)^3} |\boldsymbol{q}_j\rangle\langle\boldsymbol{q}_j|$$

bare state label

Two-body channel label

$$1 = \sum_{a} (\psi|\psi_a\rangle\langle\psi_a|\psi) + \sum_{j} \int \frac{d^3q}{(2\pi)^3} (\psi|\boldsymbol{q}_j\rangle\langle\boldsymbol{q}_j|\psi) = \sum_{a} Z_a + \sum_{j} X_j$$

elementariness of bare state a

Compositeness of channel j

$$X_j = -\underline{g_j^2} \left[\frac{dG_j}{dE}\right]_{E=M_{\mathrm{R}}-i\Gamma_{\mathrm{R}}/2} \quad \text{with} \quad G_j = \int \frac{d^3q}{(2\pi)^3} \frac{[f(q)]^2}{E - E_{j1} - E_{j2}} =$$

residue

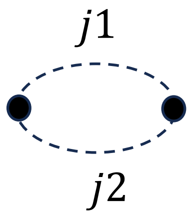

Caveat on compositeness

$$X_j = -\underbrace{g_j^2}_{\text{residue}} \left[\frac{dG_j}{dE} \right]_{E = M_{\mathrm{R}} - i\Gamma_{\mathrm{R}}/2} \quad \text{with} \quad G_j = \int \frac{d^3q}{(2\pi)^3} \frac{[f(q)]^2}{E - E_{j1} - E_{j2}} \quad =$$

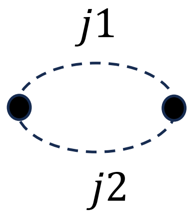

- Compositeness depends on form factors (model dependent)

  → model-independent at shallow bound state limit (*X* can be expressed with scattering length)

- For p-wave channels ($D\bar{D}, D^*\bar{D}$, $D^*\bar{D}^*$, etc.), more dependent on form factor
- Difficult to interpret Im[X], X < 0, X >1
- When | Im[X] | << 1, 0 < X < 1, compositeness may suggest hadron-molecule contents in resonance

Pole locations

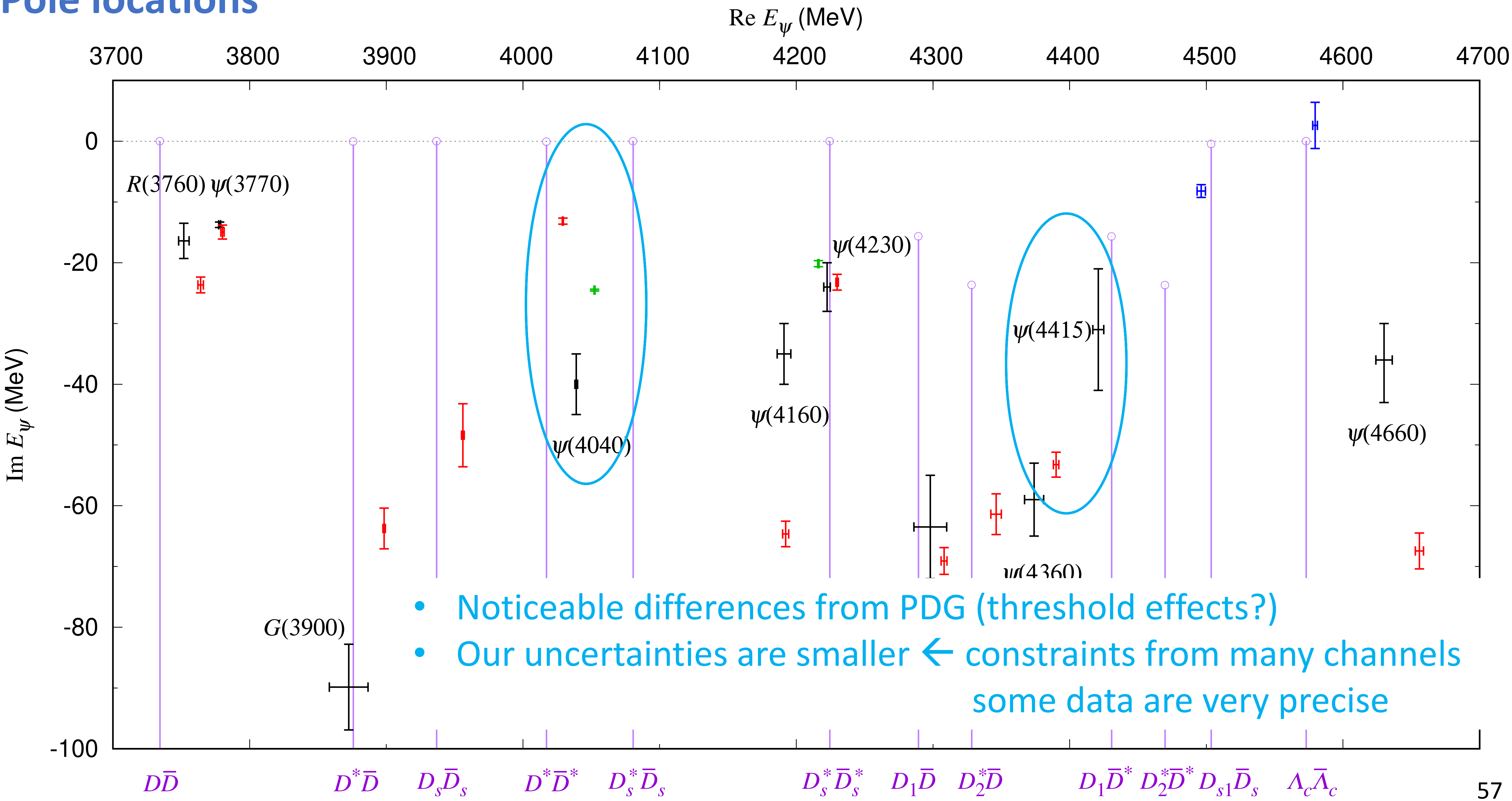

- Noticeable differences from PDG (threshold effects?)
- Our uncertainties are smaller ← constraints from many channels
  some data are very precise

Pole locations

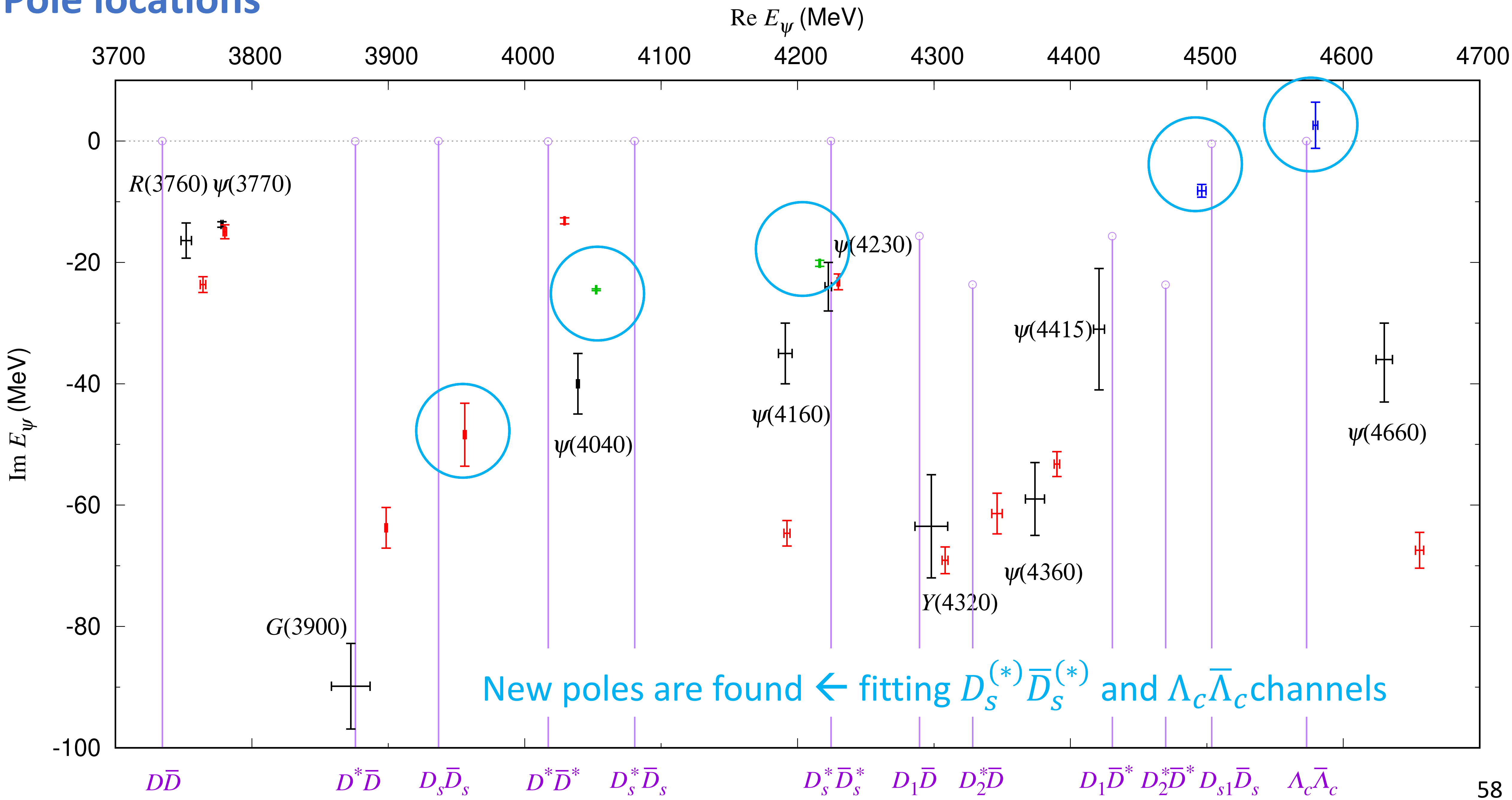

New poles are found ← fitting $D_s^{(*)}\bar{D}_s^{(*)}$ and $\Lambda_c\bar{\Lambda}_c$ channels

Pole locations (no coupling to bare ψ)

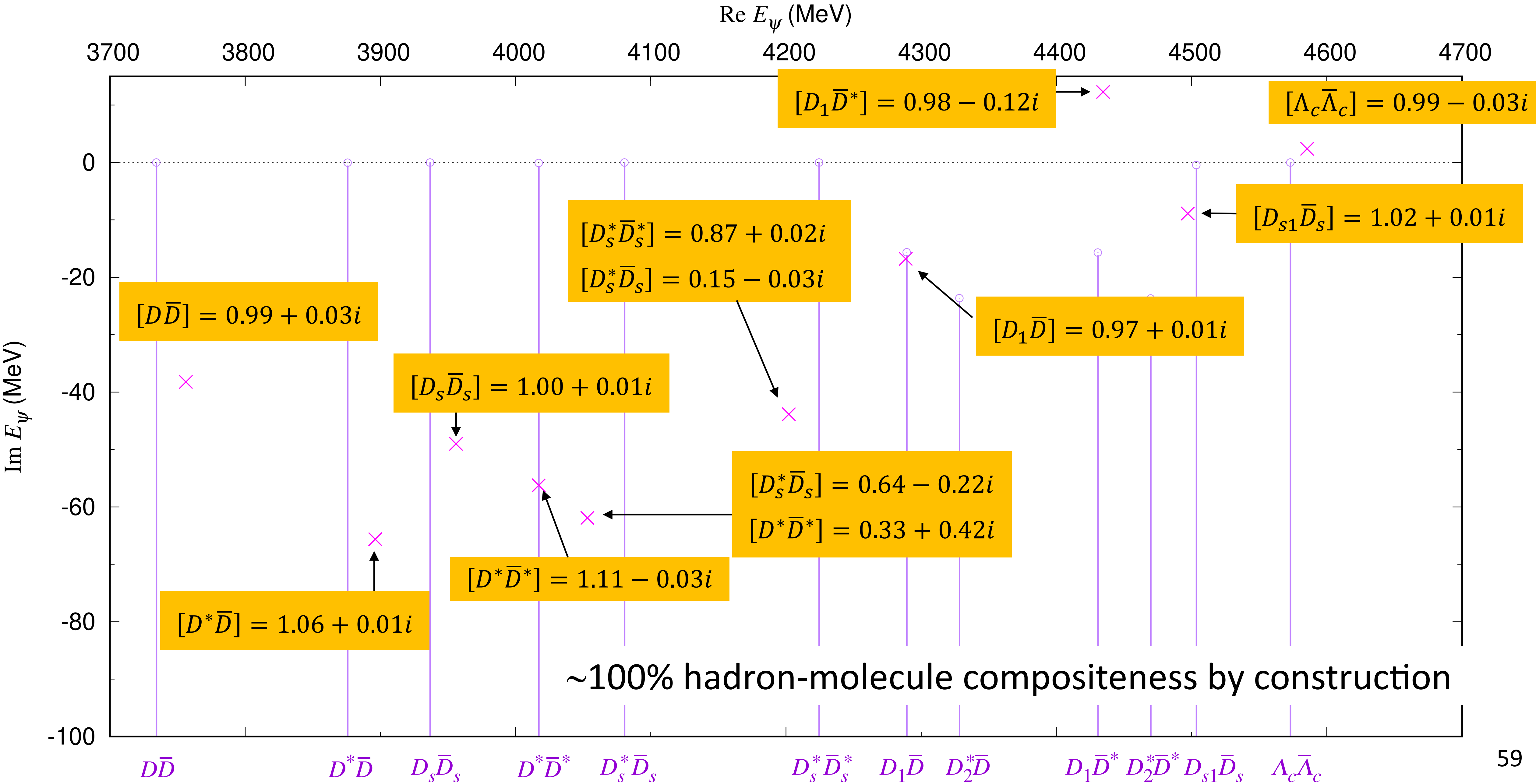

$[D_1\bar{D}^*] = 0.98 - 0.12i$

$[\Lambda_c\bar{\Lambda}_c] = 0.99 - 0.03i$

$[D_{s1}\bar{D}_s] = 1.02 + 0.01i$

$[D_s^*\bar{D}_s^*] = 0.87 + 0.02i$

$[D_s^*\bar{D}_s] = 0.15 - 0.03i$

$[D\bar{D}] = 0.99 + 0.03i$

$[D_1\bar{D}] = 0.97 + 0.01i$

$[D_s\bar{D}_s] = 1.00 + 0.01i$

$[D_s^*\bar{D}_s] = 0.64 - 0.22i$

$[D^*\bar{D}^*] = 0.33 + 0.42i$

$[D^*\bar{D}^*] = 1.11 - 0.03i$

$[D^*\bar{D}] = 1.06 + 0.01i$

~100% hadron-molecule compositeness by construction

Pole trajectories (0 → full coupling to bare ψ)

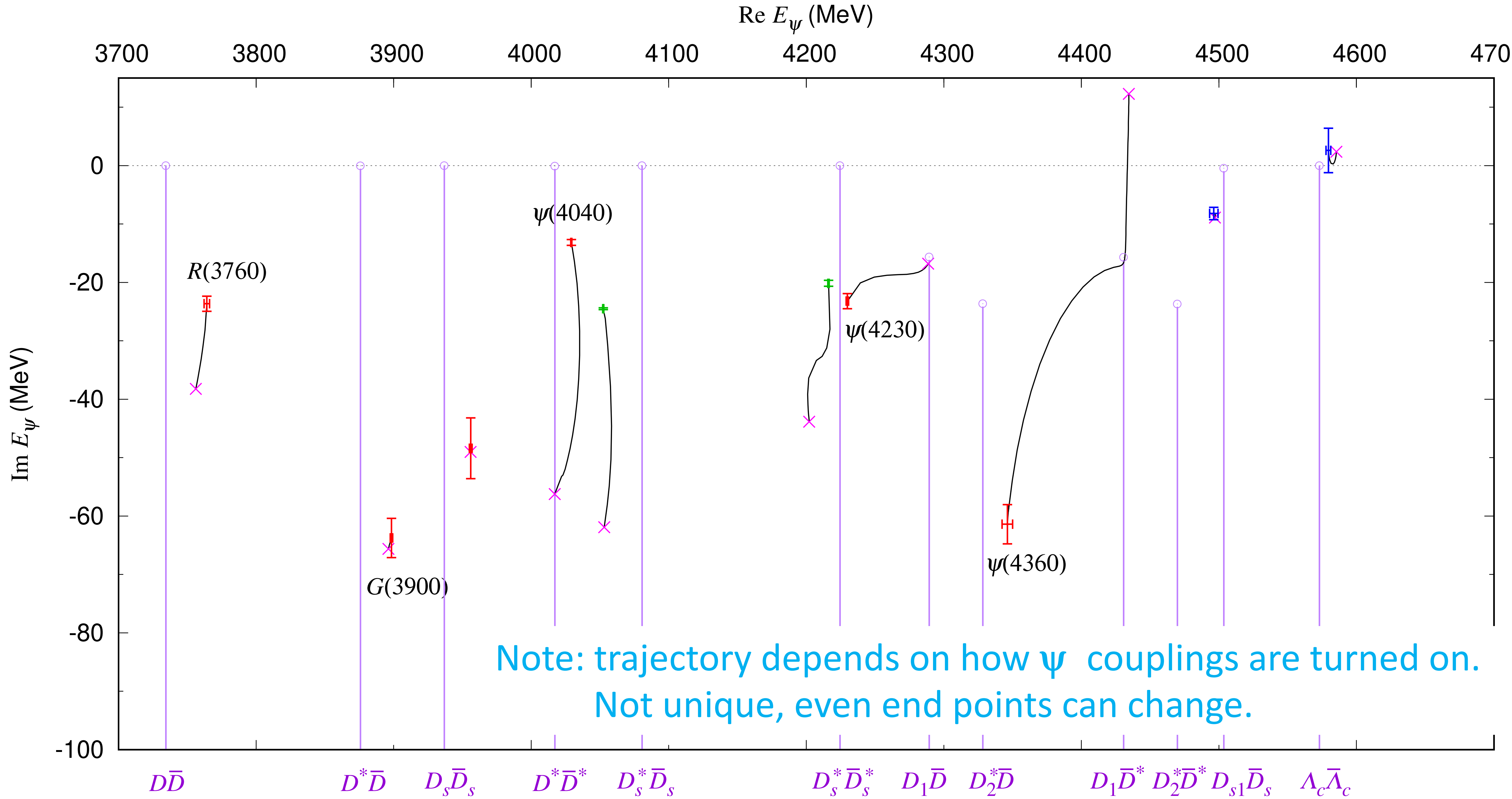

Note: trajectory depends on how ψ couplings are turned on.
Not unique, even end points can change.

Compositeness

$c\bar{c}$ dominated states

$\psi(3770)\ \ [D\bar{D}] = -0.66 - 0.41i \qquad \rightarrow\ [c\bar{c}] \sim 1.7$

$\psi(4160)\ \ [D^*\bar{D}^*] = 0.26 - 0.03i$

$[D_1\bar{D}] = 0.01 - 0.02i \qquad \rightarrow\ [c\bar{c}] \sim 0.85$

$[D_s^*\bar{D}_s^*] = -0.10 - 0.04i$

$\mathrm{Y}(4320)\ \ [D^*\bar{D}^*] = 0.02 - 0.15i$

$[D_s^*\bar{D}_s] = 0.05 + 0.06i \qquad \rightarrow\ [c\bar{c}] \sim 1.06$

$[D_s^*\bar{D}_s^*] = -0.11 - 0.03i$

$\psi(4415)\ \ [D_1\bar{D}] = -0.03 + 0.04i$

$[D_1\bar{D}^*] = 0.08 + 0.13i \qquad \rightarrow\ [c\bar{c}] \sim 0.90$

$[D_2^*\bar{D}^*] = 0.06 - 0.03i$